Article:

Pickup, B.T. orcid.org/0000-0002-2728-5486, Fowler, P.W. and Sciriha, I. (2016) A Hückel source-sink-potential theory of Pauli spin blockade in molecular electronic devices. Journal of Chemical Physics, 145 (20). 204113. ISSN 0021-9606

https://doi.org/10.1063/1.4967957

A Hückel Source-Sink-Potential theory of Pauli Spin Blockade in molecular electronic devices

Barry T. Pickup,[1, a)] Patrick W. Fowler,[1, b)] and Irene Sciriha[2]

[1)] *Department of Chemistry, University of Sheffield, Sheffield, S3 7HF, UK*

[2)] *Department of Mathematics, University of Malta, Msida, MSD 2080, Malta*[c)]

(Dated: 2016/10/19 at time 10:45:15)

This paper shows how to include Pauli (Exclusion Principle) effects within a treatment of ballistic molecular conduction that uses the tight-binding Hückel Hamiltonian and the source-sink-potential (SSP) method. We take into account the many-electron ground-state of the molecule and show that we can discuss ballistic conduction for a specific molecular device in terms of four structural polynomials. In the standard one-electron picture, these are characteristic polynomials of vertex-deleted graphs, with spectral representations in terms of molecular-orbital eigenvectors and eigenvalues. In a more realistic many-electron picture, the spectral representation of each polynomial is retained but projected into the manifold of unoccupied spin-orbitals. Crucially, this projection preserves interlacing properties. With this simple reformulation, selection rules for device transmission, expressions for overall transmission, and partition of transmission into bond currents can all be mapped onto the formalism previously developed. Inclusion of Pauli Spin Blockade, in the absence of external perturbations, has a generic effect (suppression of transmission at energies below the Fermi level) and specific effects at anti-bonding energies, which can be understood using our previous classification of inert and active shells. The theory predicts the intriguing phenomenon of Pauli Perfect Reflection whereby, once a critical electron count is reached, some electronic states of devices can give total reflection of electrons at *all* energies.

[a)] corresponding author; Electronic mail: B.T.Pickup@sheffield.ac.uk

[b)] corresponding author; Electronic mail: P.W.Fowler@sheffield.ac.uk

[c)] Electronic mail: irene.sciriha-aquilina@um.edu.mt

I. INTRODUCTION

Single molecules might be regarded as the ultimate goal in the miniaturisation of the transistor. The first theoretical paper on conduction through molecules was published by Aviram and Ratner in 1974,[1] who suggested that a single molecule could act as a rectifier. Many papers have been published since, and the principal tool for theoretical understanding has been the non-equilibrium Green's function approach.[2] A recent review of forty years of progress in the area has been given by Ratner.[3] The research literature continues to expand rapidly,[4–6] with frequent special issues of journals[7–9] and numerous books[10,11] dedicated to the topic.

The present work uses the Hückel (tight-binding) approximation to study the ballistic conduction of electrons through molecules, *i.e.* elastic scattering with no transfer of energy to or from the target molecule. We use the source-sink-potential method (SSP),[12] an approach that allows the modelling of a device comprising a molecule and two extra 'atoms', the source and the sink (*c.f.* Fig. 1). The source mimics the effect of a stream of electrons of energy ε carried by a semi-infinite wire, which is partly reflected and partly transmitted by the molecule of interest. The sink mimics a semi-infinite wire carrying away the transmitted electrons at the same energy.

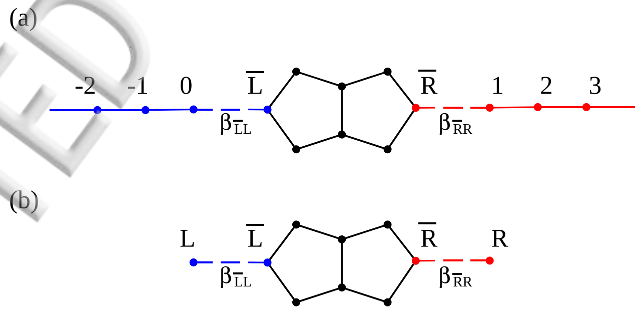

FIG. 1. a) A molecule attached to infinite left- and right-hand wires, showing the numbering scheme adopted for the atoms in the wires. b)The corresponding SSP molecular device comprising a molecule attached to source and sink atoms L and R *via* molecular contacts L̄ and R̄, respectively.

The overall transmission of an SSP device based on a molecular graph, G, with connections $\bar{\mathrm{L}}$ and $\bar{\mathrm{R}}$ is[13]

$$T(\varepsilon) = \mathcal{B}(q_{\mathrm{L}}, q_{\mathrm{R}}) \frac{j^2}{|D|^2}, \tag{1}$$

where ε is the energy of the incoming electronsl. The band-pass function, which ensures that the electron energy is within the conduction band of the wire, is

$$\mathcal{B}(q_{\mathrm{L}}, q_{\mathrm{R}}) = (2\beta_{\mathrm{L}} \sin q_{\mathrm{L}})(2\beta_{\mathrm{R}} \sin q_{\mathrm{R}})\beta_{\bar{\mathrm{L}}\mathrm{L}}^2 \beta_{\bar{\mathrm{R}}\mathrm{R}}^2. \tag{2}$$

The polynomial occurring in the numerator is

$$\jmath(\varepsilon) = (-1)^{\bar{\mathrm{L}}+\bar{\mathrm{R}}} \det\left(\varepsilon\mathbf{1} - \mathbf{A}\right)^{[\bar{\mathrm{L}},\bar{\mathrm{R}}]} \tag{3}$$

where row $\bar{\mathrm{L}}$ and column $\bar{\mathrm{R}}$ have been removed from the determinant of the characteristic matrix $\varepsilon\mathbf{1} - \mathbf{A}$, in which $\mathbf{A}$ is the adjacency matrix of G. The denominator of Eq. (1) depends on

$$\begin{aligned} D(\varepsilon) = {}& \beta_{\mathrm{L}} e^{-iq_{\mathrm{L}}} \beta_{\mathrm{R}} e^{-iq_{\mathrm{R}}} s - \beta_{\mathrm{R}} e^{-iq_{\mathrm{R}}} \beta_{\bar{\mathrm{L}}\mathrm{L}}^2 t \\ & - \beta_{\mathrm{L}} e^{-iq_{\mathrm{L}}} \beta_{\bar{\mathrm{R}}\mathrm{R}}^2 u + \beta_{\bar{\mathrm{L}}\mathrm{L}}^2 \beta_{\bar{\mathrm{R}}\mathrm{R}}^2 v, \end{aligned} \tag{4}$$

Here, all β integrals are defined in Fig 1. The wave-vectors q_{L} and q_{R} are functions of ε obeying the dispersion relations

$$\varepsilon = \alpha_{\mathrm{L}} + 2\beta_{\mathrm{L}} \cos q_{\mathrm{L}} = \alpha_{\mathrm{R}} + 2\beta_{\mathrm{R}} \cos q_{\mathrm{R}}. \tag{5}$$

with Hückel parameters $(\alpha_{\mathrm{L}}, \beta_{\mathrm{L}})$ and $(\alpha_{\mathrm{R}}, \beta_{\mathrm{R}})$, for left and right wires, respectively. The four *structural polynomials*,[13] s, t, u, and v, are defined as

$$\begin{aligned} s(\varepsilon) &= \det\left(\varepsilon\mathbf{1} - \mathbf{A}\right), \\ t(\varepsilon) &= \det\left(\varepsilon\mathbf{1} - \mathbf{A}\right)^{[\bar{\mathrm{L}},\bar{\mathrm{L}}]}, \\ u(\varepsilon) &= \det\left(\varepsilon\mathbf{1} - \mathbf{A}\right)^{[\bar{\mathrm{R}},\bar{\mathrm{R}}]}, \\ v(\varepsilon) &= \det\left(\varepsilon\mathbf{1} - \mathbf{A}\right)^{[\bar{\mathrm{L}}\bar{\mathrm{R}},\bar{\mathrm{L}}\bar{\mathrm{R}}]}. \end{aligned} \tag{6}$$

The superscripts in Eq. (6) indicate which rows and columns corresponding to connection atoms $\bar{\mathrm{L}}$ and/or $\bar{\mathrm{R}}$ are to be struck out from the characteristic matrix. The *fifth* polynomial, appearing in the numerator of Eq. (1), and defined in Eq. (3) satisfies the Jacobi-Sylvester relation[14]

$$\jmath^2 = ut - sv, \tag{7}$$

and so the entire function, $T(\varepsilon)$ can be reconstructed from characteristic polynomials of four graphs: those of the molecule, the molecule minus each connection, and the molecule minus both connections.

Using this approach, we have been able to classify conduction/insulation properties of molecules in terms of 11 cases depending on the interlacing properties of the structural polynomials.[15,16]

More recently, we have reformulated the SSP method to give a more detailed account,[17] in which the equations are written in the molecular-orbital basis. In this representation, conduction through the molecule can be viewed as occurring through parallel molecular-orbital channels or, more precisely, through shells of orbitals. It is found that individual shells may be conductively *inert*, *i.e.* insulating at all electron energies, ε. At the eigenvalue of an *active* (conducting) shell, all current passes through that shell. At the eigenvalue of an inert shell, current (if any) passes entirely through other shells. This rich behaviour is determined by the rank of the shell connection matrix, that portion of the SSP secular matrix describing the connection of the molecular orbitals in the shell to the source and sink atoms.

This molecular-orbital picture is appealing, but has usually been applied to molecules that are 'empty' of electrons, in the sense that all molecular-orbital channels are left open to the incoming electron. Real molecules, on the other hand, have occupied molecular orbitals, and therefore some closed channels. This paper explores how the picture can be extended to include these molecular electrons, while retaining the advantages of the previously defined formalism.[17]

The phenomenon of Pauli Spin Blockade has been recognised in the field of quantum dots[18,19] as an effect that limits electron current in situations where electrons can jump between dots that already contain filled electronic levels. Pauli Spin Blockade (PSB) was identified in Ref. 18. As Perron *et al.* note, PSB has played a useful role in investigations of the physics of spin-to-charge conversion.[20] PSB has implications for spin relaxation times,[21,22] coupling of electron spin to nuclear lattices,[23] spin-orbit coupling,[24] and spintronics.[25–27] The Pauli Spin Blockade effect has also been noted by Ernzerhof *et al.*[28,29] who applied the SSP method to molecular conduction, introducing electronic interactions by means of the Hubbard interaction.[30] In the present work, we do not consider electron-electron repulsion directly, but concentrate instead on the effects of Pauli fermion statistics on non-interacting many-electron states: these lead to the closing down of conduction channels associated with energies below the Fermi level. Further effects, in which Pauli Spin Blockade may be lifted, or even reversed, depend on the application of external magnetic fields, not yet included in the present treatment.[20,31–34]

The plan of the remainder of this paper is as follows. Sec. II gives a brief derivation of the SSP equations for a many-electron molecule in the tight-binding approximation. In Sec. III we derive expressions for total transmission and shell currents allowing for the effects of the Pauli principle. The reader who wishes to skip the details of the derivations, may turn directly to Sec. IV. The central results given in this section (IV B) are the tables of conduction cases in which it is shown that the selection rules for ballistic molecular conduction extend easily to the new model, giving the possibility of pencil-and-paper calculation of conduction/insulation for any given molecular device. The following section on new behaviour arising from the presence of molecular electrons describes the main physical consequences of inclusion of Pauli effects, *viz.* Pauli Spin Blockade, and Pauli Total Reflection. A brief examples section illustrates the working of the general theory (Sec. VI) in some typical cases. Finally, conclusions (Sec. VII), are drawn and some directions for extension of the model are indicated.

II. THE SSP METHOD

Our treatment concentrates attention on the molecule. We allow for a single scattering electron passing through the wires. There is no explicit electron-electron interaction in the Hückel tight-binding model, and so all many-electron effects within the model arise from the Fermi statistics. In this treatment, the many-electron part of the wave-function is localised on the molecule, and the N electrons inside the molecule, apart from their statistical effect, are passive spectators to ballistic conduction.

Derivation of the SSP equations for the ballistic current proceeds by defining the wave-function within the molecule (section II A), and within the leads (Sec. II B), and then using complex scattering potentials to enforce the boundary conditions for our finite model of the device (Sec. II C).

A. Wave-functions inside the isolated molecule

We use a set of $2p_z$ atomic basis functions on the atoms of the molecular π-system, $\{\phi_{\mathrm{p}}\}$, where $p = 1, 2, \ldots, n$. In Hückel theory, this is taken to be an orthonormal basis

$$\langle \phi_{\mathrm{p}} \mid \phi_{\mathrm{q}} \rangle = \delta_{\mathrm{pq}}. \tag{8}$$

Assuming, for simplicity, a pure carbon skeleton, the matrix elements over the Hückel Hamiltonian are

$$\begin{aligned} \mathrm{h}_{\mathrm{pp}} &=< \phi_{\mathrm{p}} \mid \hat{h} \mid \phi_{\mathrm{p}} >= \alpha = 0, \\ \mathrm{h}_{\mathrm{pq}} &=< \phi_{\mathrm{p}} \mid \hat{h} \mid \phi_{\mathrm{q}} >= \begin{cases} \beta = \ \ 1 & \text{for p} \sim \text{q} \\ \quad\ \ 0 & \text{otherwise} \end{cases} \end{aligned} \tag{9}$$

where we have used the convention that α defines the origin and and β the unit of the energy scale. We can define a set of molecular orbitals satisfying the *one-electron* Hückel secular equations

$$\hat{h}\psi_{\mathrm{k}} = \epsilon_{\mathrm{k}}\psi_{\mathrm{k}}. \tag{10}$$

The molecular orbitals can be expanded in the basis as

$$\psi_{\mathrm{k}} = \sum_{\mathrm{p}=1}^{n} \phi_{\mathrm{p}} U_{\mathrm{pk}}. \tag{11}$$

where the U_{pk} are the MO coefficients. Without loss of generality, we assume the $\{U_{\mathrm{pk}}\}$ to be real throughout this paper.

We can now consider the *many-electron* Hamiltonian. Within Hückel theory this is a sum of one-electron operators,

$$\hat{H} = \sum_{i=1}^{N} \hat{h}_i, \tag{12}$$

where $\hat{\mathrm{h}}_i$ acts upon electron i only.

To construct many-electron states we use spin-orbitals, $\psi_{\mathrm{k}\sigma_{\mathrm{k}}}$, where the suffix σ_{k} indicates that each pure spin-orbital in the Slater determinant has either α or β spin. Arbitrary electron configurations can be defined as

$$\Phi_{\mathrm{K}} = |\psi_{\mathrm{k}_1\sigma_1}\psi_{\mathrm{k}_2\sigma_2}\cdots\psi_{\mathrm{k}_N\sigma_N}|, \tag{13}$$

where the configuration function is labelled by $\mathrm{K} = \{\mathrm{k}_1\sigma_1, \mathrm{k}_2\sigma_2, \cdots, \mathrm{k}_N\sigma_N\}$. The N-electron states constructed from orbitals satisfying Eq. (10) form an orthonormal set that diagonalises the many-electron Hamiltonian:

$$\begin{aligned} < \Phi_{\mathrm{K}} \mid \hat{H} \mid \Phi_{\mathrm{K}'} > &= \delta_{\mathrm{K},\mathrm{K}'} E_{\mathrm{K}}, \\ < \Phi_{\mathrm{K}} \mid \Phi_{\mathrm{K}'} > &= \delta_{\mathrm{K},\mathrm{K}'}, \end{aligned} \tag{14}$$

where

$$E_{\mathrm{K}} = \sum_{\mathrm{k}\in K} \epsilon_{\mathrm{k}}. \tag{15}$$

Our model for the molecule uses a molecular ground-state configuration described by a product of the N molecular spin-orbitals of lowest energy

$$\Phi_0 = |\psi_{1\sigma_1}\psi_{2\sigma_2}\cdots\psi_{N\sigma_N}|, \tag{16}$$

with

$$E_0 = \sum_{\mathrm{k}=1}^{N} \epsilon_{\mathrm{k}}. \tag{17}$$

In general, the numbers of α and β spins in the molecular ground state configuration are not equal. In contrast with the one-electron picture, therefore, transmission can be different for incoming electrons of each spin: to acknowledge this new feature, the transmission function $T(\varepsilon)$ in the SSP model will now be denoted $T_\sigma(\varepsilon)$, where σ is the spin of the electron on the wire. For closed-shell molecules the ground-state will have spin-paired, doubly-occupied orbitals. We allow arbitrary spin states here, as many molecules have open-shell ground-states. In the following sections we adopt a notation in which unoccupied MOs are labelled $\psi_{\mathrm{a}}, \psi_{\mathrm{b}}, \ldots$.

B. Wave-functions inside the wires

We wish to describe a single continuum electron passing down semi-infinite wires, with N-electrons residing in the molecule. We can write these scattering wave-functions on the wires in terms of $(N+1)$-electron configurations as $\Phi_0^{q_{\mathrm{L}}\sigma}, \Phi_0^{q_{\mathrm{R}}\sigma}$ in the left- and right-hand wires, respectively, *i.e.*

$$\Phi_0^{q_\mathrm{L}\sigma} = \sum_{\mathrm{w}=-\infty}^{0} C_\mathrm{w} \Phi_0^{\mathrm{w}\sigma},$$
$$\Phi_0^{q_\mathrm{R}\sigma} = \sum_{\mathrm{w}=1}^{\infty} C_\mathrm{w} \Phi_0^{\mathrm{w}\sigma}, \tag{18}$$

where

$$\Phi_0^{\mathrm{w}\sigma} = |\phi_{\mathrm{w}\sigma}\psi_{1\sigma_1}\psi_{2\sigma_2}\cdots\psi_{N\sigma_N}| \tag{19}$$

are left- or right-wire configuration functions and the $\phi_{\mathrm{w}\sigma}$ are spin-orbital basis functions with spin σ on the atoms of left and right wires, depending on the index w shown in Fig. 1b. We note that the energy associated with the scattering states, $\Phi_0^{\mathrm{qL}\sigma}$, $\Phi_0^{\mathrm{qR}\sigma}$, is required to be the $(N+1)$-electron energy E, where

$$E = \langle \Phi_0^{q_\mathrm{L}\sigma} \mid \hat{H} \mid \Phi_0^{q_\mathrm{L}\sigma} \rangle = \langle \Phi_0^{q_\mathrm{R}\sigma} \mid \hat{H} \mid \Phi_0^{q_\mathrm{R}\sigma} \rangle$$
$$= E_0 + \varepsilon \tag{20}$$

in terms of the molecular ground-state energy, E_0, and the energy of a single scattering electron, ε. Coefficients satisfying the tight-binding secular equations on the wires are

$$C_\mathrm{w} = \frac{1}{N_\mathrm{L}}\left(e^{iq_\mathrm{L}\mathrm{w}} + re^{-iq_\mathrm{L}\mathrm{w}}\right) \text{ for } \mathrm{w} = -\infty, \ldots, 1, 0,$$
$$C_\mathrm{w} = \frac{1}{N_\mathrm{R}}\tau e^{iq_\mathrm{R}\mathrm{w}} \text{ for } \mathrm{w} = 1, 2, \ldots, \infty. \tag{21}$$

The left-hand wave-function combines a forward-travelling wave (e^{iq_L}) and a backward-travelling wave (e^{-iq_L}) with a reflection coefficient, r. The molecule acts as a potential barrier that produces a reflected wave in the left wire and a forward transmitted wave (e^{iq_R}) in the right wire, with a transmission coefficient, τ. This corresponds to a flux of electrons with energy ε, satisfying energy conservation and the Hückel Schrödinger equation for infinite wires.

The total electron transmission probability is

$$T_\sigma(\varepsilon) = 1 - |r|^2 = |\tau|^2 \tag{22}$$

Normalisation factors N_L and N_R have been introduced to obtain the requisite unit electron flux. Hence, the current density[35] from atom $(\mathrm{w}-1)$ to atom w in the left wire, using the standard Hückel formulation, is

$$J^{\text{left}}_{(\text{w}-1)\to\text{w}} = \frac{1}{i}\left(\left\langle \Phi_0^{\text{w}-1\sigma}|\hat{H}|\Phi_0^{\text{w}\sigma}\right\rangle C_{\text{w}-1}C_{\text{w}} - \text{c.c.}\right) \\ = \frac{2\beta_{\text{L}}\sin q_{\text{L}}}{N_{\text{L}}^2}\left(1-|r|^2\right), \tag{23}$$

where we have used Slater's rules

$$< \Phi_0^{\text{w}-1\sigma}|\hat{H}|\Phi_0^{\text{w}\sigma} >=< \phi_{\text{w}-1}|\hat{h}|\phi_{\text{w}} >= \beta_{\text{L}}. \tag{24}$$

The expression in Eq. (23) is independent of the index w, showing that a constant current flows down the wire. We require this current to be equal to the transmission probability, $T_\sigma(\varepsilon)$. Hence, the correct flux normalisation is achieved by setting

$$N_{\text{L}}^2 = 2\beta_{\text{L}}\sin q_{\text{L}}, \tag{25}$$

and, for the right-hand wire,

$$N_{\text{R}}^2 = 2\beta_{\text{R}}\sin q_{\text{R}}. \tag{26}$$

C. The many-electron SSP equations

The $(N+1)$-electron configurations, $\Phi_0^{\text{w}\sigma}$, describe configurations having one electron in one or other of the wires and N-electrons in the molecule. For electron transmission to occur, these configuration functions must interact with appropriate configurations in which all electrons are on the molecule. These configurations must be single excitations relative to $\Phi_0^{\text{w}\sigma}$. Such configuration functions are of the form

$$\Phi_0^{\text{a}\sigma} = |\psi_{\text{a}\sigma}\psi_{1\sigma_1}\psi_{2\sigma_2}\dots\psi_{N\sigma_N}| \tag{27}$$

for $\text{a} = N+1, N+2, \dots, n$, and all have an extra electron with the same spin. We write the many-electron device wave-function as

$$\Psi^{dev} = \sum_{\text{w}=-\infty}^{0} C_{\text{w}}\Phi_{\text{w}\sigma} + \sum_{\text{a}=N+1}^{n} C_{\text{a}}\Phi_0^{\text{a}\sigma} + \sum_{\text{w}=1}^{\infty} C_{\text{w}}\Phi_{\text{w}\sigma}, \tag{28}$$

where the three terms describe a scattering electron in the left wire, an extra electron passing through the molecule, and a scattering electron in the right wire. All terms describe N passive electrons present in the occupied orbitals of a molecule. This description is consistent with the absence of two-electron interactions within the Hückel model.

The secular equations of the device shown in Fig. 1b, for atom 0 in the left-hand wire and for atom 1 in the right-hand wire, are

$$
\begin{aligned}
H_{0,-1}C_{-1} + \left(H_{0,0} - E\right) C_0 + \sum_{\mathrm{a}} H_{0,a}C_a &= 0, \\
\sum_{\mathrm{a}} H_{1,a}C_a + \left(\hat{H}_{1,1} - E\right) C_1 + H_{1,2}C_2 &= 0,
\end{aligned} \tag{29}
$$

where the CI matrix elements are

$$
\begin{aligned}
H_{0,-1} &= \langle \Phi_0^{0\sigma} \mid \hat{H} \mid \Phi_0^{-1\sigma} \rangle = \langle \phi_0 \mid \hat{h} \mid \phi_{-1} \rangle = \beta_{\mathrm{L}}, \\
H_{0,0} &= \langle \Phi_0^{0\sigma} \mid \hat{H} \mid \Phi_0^{0\sigma} \rangle \;\; = \langle \phi_0 \mid \hat{h} \mid \phi_0 \rangle \;\; = \alpha_{\mathrm{L}} + E_0, \\
H_{0,a} &= \langle \Phi_0^{0\sigma} \mid \hat{H} \mid \Phi^{a\sigma} \rangle \;\; = \langle \phi_0 \mid \hat{h} \mid \psi_{\mathrm{a}} \rangle \;\; = \beta_{\bar{\mathrm{L}}\mathrm{L}} U_{\bar{\mathrm{L}}\mathrm{a}}, \\
H_{1,a} &= \langle \Phi_0^{1\sigma} \mid \hat{H} \mid \Phi^{a\sigma} \rangle \;\; = \langle \phi_1 \mid \hat{h} \mid \psi_{\mathrm{a}} \rangle \;\; = \beta_{\bar{\mathrm{R}}\mathrm{R}} U_{\bar{\mathrm{R}}\mathrm{a}}, \\
H_{1,1} &= \langle \Phi_0^{1\sigma} \mid \hat{H} \mid \Phi_0^{1\sigma} \rangle \;\; = \langle \phi_1 \mid \hat{h} \mid \phi_1 \rangle \;\; = \alpha_{\mathrm{R}} + E_0, \\
H_{1,2} &= \langle \Phi_0^{1\sigma} \mid \hat{H} \mid \Phi_0^{2\sigma} \rangle \;\; = \langle \phi_1 \mid \hat{h} \mid \phi_2 \rangle \;\; = \beta_{\mathrm{R}},
\end{aligned} \tag{30}
$$

and $\beta_{\bar{\mathrm{L}}\mathrm{L}}, \beta_{\bar{\mathrm{R}}\mathrm{R}}$ are resonance parameters for the connections from the wires to the molecule. We wish to replace the left wire by a single source atom, L, sited at atom 0 and creating a flux of electrons corresponding to the wave-function Φ_0^{qL} in Eqs. (18, 21). Similarly, we wish to replace the right wire by a single sink atom, R sited at atom 1 and removing the transmitted flux. This is achieved by definition of *complex* potentials, $\Theta_{\mathrm{L}}, \Theta_{\mathrm{R}}$,[12] on these source and sink atoms to replace the effects of all atoms to the left of atom 0, and all to the right of atom 1, respectively. Hence, we define

$$
\begin{aligned}
\beta_{\mathrm{L}} C_{-1} &= \Theta_{\mathrm{L}} C_0, \\
\beta_{\mathrm{R}} C_2 &= \Theta_{\mathrm{R}} C_1.
\end{aligned} \tag{31}
$$

The potentials can now be derived by using the expressions from Eq. (21) for the orbital coefficients

$$
\begin{aligned}
\Theta_{\mathrm{L}} &= \beta_{\mathrm{L}} \frac{C_{-1}}{C_0} = \beta_{\mathrm{L}} \frac{\left(e^{-iq_{\mathrm{L}}} + r e^{iq_{\mathrm{L}}}\right)}{(1+r)}, \\
\Theta_{\mathrm{R}} &= \beta_{\mathrm{R}} \frac{C_2}{C_1} = \beta_{\mathrm{R}} e^{iq_{\mathrm{R}}}.
\end{aligned} \tag{32}
$$

In the standard SSP formalism[13,36,37] these potentials are used directly in the SSP secular equations. However, when the reflection coefficient r becomes equal to -1, the potential Θ_{L}

becomes infinite. A more satisfactory approach, avoiding this singularity,[17] is obtained by substituting the explicit form of the orbital coefficient C_{-1} into Eq. (29), to give

$$\frac{\beta_{\mathrm{L}}}{N_{\mathrm{L}}}\left(e^{-iq_{\mathrm{L}}}+re^{iq_{\mathrm{L}}}\right)+\left(\alpha_{\mathrm{L}}+E_0-E\right)C_{\mathrm{L}}+\beta_{\bar{\mathrm{L}}\mathrm{L}}C_{\bar{\mathrm{L}}}=0. \tag{33}$$

Noting from Eq. (21) that the source coefficient is

$$C_{\mathrm{L}}\equiv C_0=\frac{1+r}{N_{\mathrm{L}}}, \tag{34}$$

we deduce that

$$r=N_{\mathrm{L}}C_{\mathrm{L}}-1. \tag{35}$$

Substituting for r in Eq. (33), we obtain

$$\begin{aligned}\left(\beta_{\mathrm{L}}e^{iq_{\mathrm{L}}}+\alpha_{\mathrm{L}}+E_0-E\right)C_{\mathrm{L}}+\beta_{\bar{\mathrm{L}}\mathrm{L}}C_{\bar{\mathrm{L}}}&=\frac{2i\beta_{\mathrm{L}}\sin q_{\mathrm{L}}}{N_{\mathrm{L}}}\\&=iN_{\mathrm{L}},\end{aligned} \tag{36}$$

where we have placed the inhomogeneity term on the right-hand side. We can carry out the same procedure using C_1 from Eq. (21) in Eq. (29) to give the sink coefficient

$$C_{\mathrm{R}}\equiv C_1=\frac{\tau}{N_{\mathrm{R}}}e^{iq_{\mathrm{R}}}, \tag{37}$$

and hence

$$C_2=e^{2iq_{\mathrm{R}}}\frac{\tau}{N_{\mathrm{R}}}=e^{iq_{\mathrm{R}}}C_{\mathrm{R}}. \tag{38}$$

Substitution of this expression into Eq. (29) gives

$$\beta_{\bar{\mathrm{R}}\mathrm{R}}C_{\bar{\mathrm{R}}}+\left(\alpha_{\mathrm{R}}+E_0-E+\beta_{\mathrm{R}}e^{iq_{\mathrm{R}}}\right)C_{\mathrm{R}}=0 \tag{39}$$

which does not contain an inhomogeneity.

With these modifications to the boundary conditions, we can now find the wave-function for the SSP model device. The wave-function

$$\Psi^{\mathrm{SSP}}=C_{\mathrm{L}}\Phi_0^{\mathrm{L}\sigma}+\sum_{\mathrm{a}=N+1}^{n}C_{\mathrm{a}}\Phi_0^{\mathrm{a}\sigma}+C_{\mathrm{R}}\Phi_0^{\mathrm{R}\sigma} \tag{40}$$

is the solution to the SSP equations in the CI formalism. The $\Phi^{\mathrm{a}\sigma}$ here are configurations with $N+1$ electrons in the molecule, and $\Phi^{\mathrm{L}\sigma}$, $\Phi^{\mathrm{R}\sigma}$ have an extra electron on source or sink atoms, respectively. The $(n+2)$-dimensional SSP equations for the SSP device depicted in Fig. 1a can now be written in matrix form as

$$\mathbf{P}\begin{pmatrix}\mathbf{C}\\ C_{\mathrm{L}}\\ C_{\mathrm{R}}\end{pmatrix}=\begin{pmatrix}\mathbf{0}\\ -iN_{\mathrm{L}}\\ 0\end{pmatrix}, \tag{41}$$

where the *device matrix* is

$$\mathbf{P}=\begin{pmatrix}\mathbf{p} & -\mathbf{u}_{\mathrm{L}} & -\mathbf{u}_{\mathrm{R}}\\ -\widetilde{\mathbf{u}}_{\mathrm{L}} & \varepsilon-\alpha_{\mathrm{L}}-\beta_{\mathrm{L}}e^{iq_{\mathrm{L}}} & 0\\ -\widetilde{\mathbf{u}}_{\mathrm{R}} & 0 & \varepsilon-\alpha_{\mathrm{R}}-\beta_{\mathrm{R}}e^{iq_{\mathrm{R}}}\end{pmatrix}, \tag{42}$$

and the $(n-N)$-dimensional diagonal matrix

$$p_{\mathrm{ab}}=\delta_{\mathrm{ab}}(\varepsilon-\epsilon_{\mathrm{a}}), \tag{43}$$

contains only the energies of unoccupied molecular orbitals arising from the configurations $\{\Phi_0^{\mathrm{a}\sigma}\}$. For our single-atom-contact configurations the *connection* matrix elements, $(\mathbf{u}_{\mathrm{L}}\mathbf{u}_{\mathrm{R}})$, are expressed in terms of the MO coefficients, $\mathbf{U}$, for the virtual orbitals:

$$\begin{aligned}(\mathbf{u}_{\mathrm{L}})_{\mathrm{a}}&=\beta_{\bar{\mathrm{L}}\mathrm{L}}U_{\bar{\mathrm{L}}\mathrm{a}},\\ (\mathbf{u}_{\mathrm{R}})_{\mathrm{a}}&=\beta_{\bar{\mathrm{R}}\mathrm{R}}U_{\bar{\mathrm{R}}\mathrm{a}},\end{aligned} \tag{44}$$

and the source and sink matrix elements are

$$\begin{aligned}\varepsilon-\alpha_{\mathrm{L}}-\beta_{\mathrm{L}}e^{iq_{\mathrm{L}}}&=\beta_{\mathrm{L}}e^{-iq_{\mathrm{L}}},\\ \varepsilon-\alpha_{\mathrm{R}}-\beta_{\mathrm{R}}e^{iq_{\mathrm{R}}}&=\beta_{\mathrm{R}}e^{-iq_{\mathrm{R}}}.\end{aligned} \tag{45}$$

Here we have used the dispersion relations Eq. (5) to remove ε from source and sink matrix elements.

At this stage we have the working equations for the SSP model of a device, stated in terms of molecular orbital channels and depending entirely on quantities that can be obtained from a tight-binding calculation.

Physically, the equations describe a steady state current that may be called the ‘ground state channel’, in which N electrons reside in the molecule in a ground state configuration, and one electron from the left lead is scattered by the molecule. It is possible to envisage other scattering channels, in which the molecular electrons are present in excited N-electron states (or even channels with different electron numbers). In the present model, without electron-electron interactions, the configuration functions describing these other channels do not interact with those from the ground state channel. All channels, therefore, are independent, and are uncoupled from each other in our model.

The following section shows how to solve these equations in a way that retains the formalism of structural polynomials.

III. SOLUTION OF THE SSP EQUATIONS

We first look at the form of the structural polynomials defined in Eq. (6) when expressed in terms of MOs and orbital energies. It is clear that we can write

$$s(\varepsilon) = \prod_{\mathrm{k}=1}^{n} (\varepsilon - \epsilon_{\mathrm{k}}) \, . \tag{46}$$

The other structural polynomials are obtained by making a general definition in terms of the inverse of the secular matrix:

$$\hat{\jmath}_{\mathrm{pq}} = (\varepsilon - \mathbf{A})^{-1}_{\mathrm{pq}} = \sum_{\mathrm{k}=1}^{n} \frac{U_{\mathrm{pk}} U_{\mathrm{qk}}}{\varepsilon - \epsilon_{\mathrm{k}}}. \tag{47}$$

The structural polynomial related to this reduced 'hatted' quantity is

$$\jmath_{\mathrm{pq}}(\varepsilon) = s(\varepsilon) \hat{\jmath}_{\mathrm{pq}}(\varepsilon). \tag{48}$$

We recover the structural polynomials for a particular device with source and sink connected to vertices $\bar{\mathrm{L}}$, and $\bar{\mathrm{R}}$, by recognising that $t = \jmath_{\bar{\mathrm{L}}\bar{\mathrm{L}}}$, $u = \jmath_{\bar{\mathrm{R}}\bar{\mathrm{R}}}$, and $\jmath = \jmath_{\bar{\mathrm{L}}\bar{\mathrm{R}}}$. We can now use the analogy with Eq. (7) to define the remaining member of the set,

$$\hat{v} = \hat{u}\hat{t} - \hat{\jmath}^2, \tag{49}$$

in terms of the new structural polynomials.

To make the comparison explicit, we note that both the product in Eq. (46) and the summation in Eq. (48) involve *all* the MOs in the molecular spectrum. The form of these equations is important in what follows. We also note that the secular equations in Eqs. (41) and (42) correspond closely to Eqs. (31) and (32) in Pickup *et al.*,[17] with the exception that the latter depend on the *full range* of molecular orbitals, but the former contain only the *unoccupied* set.

Note that in the many-electron model, the structural polynomials have an implicit dependence on spin because the manifold of unoccupied orbitals included in their definition must be chosen to match the spin of the scattering electron. For simplicity this dependency will be suppressed in the notation.

A. Solutions away from eigenvalues

We can solve the SSP device equation Eq. (41), for energies ε away from all molecular eigenvalues, using the formula for a block partitioned inverse,

$$\begin{pmatrix} \mathbf{V} & \mathbf{W} \\ \mathbf{X} & \mathbf{Y} \end{pmatrix}^{-1} = \begin{pmatrix} \mathbf{Z}_1 & -\mathbf{V}^{-1}\mathbf{W}\mathbf{Z}_2 \\ -\mathbf{Y}^{-1}\mathbf{X}\mathbf{Z}_1 & \mathbf{Z_2} \end{pmatrix}, \tag{50}$$

where

$$\begin{aligned} \mathbf{Z}_1 &= \left(\mathbf{V} - \mathbf{W}\mathbf{Y}^{-1}\mathbf{X}\right)^{-1}, \\ \mathbf{Z}_2 &= \left(\mathbf{Y} - \mathbf{X}\mathbf{V}^{-1}\mathbf{W}\right)^{-1}, \end{aligned} \tag{51}$$

are Schur complements. We identify the block $\mathbf{V}$ as the diagonal matrix $\mathbf{p}$, $\mathbf{Y}$ as the two-dimensional source-sink block, and $\mathbf{W}$ as the connection matrix, $\mathbf{u}_{\mathrm{L}}\mathbf{u}_{\mathrm{R}}$. We can simplify this expression by noting that the matrix $\mathbf{X}\mathbf{V}^{-1}\mathbf{W}$ comprises terms such as

$$\begin{aligned} \tilde{u}_{\mathrm{L}}\left(\varepsilon\mathbf{1} - \boldsymbol{\epsilon}_{\mathrm{un}}\right)^{-1} u_{\mathrm{L}} &= \sum_{\mathrm{a}=N+1}^{n} \frac{U^2_{\bar{\mathrm{L}}\mathrm{a}}}{\varepsilon - \epsilon_{\mathrm{a}}}, \\ \tilde{u}_{\mathrm{R}}\left(\varepsilon\mathbf{1} - \boldsymbol{\epsilon}_{\mathrm{un}}\right)^{-1} u_{\mathrm{R}} &= \sum_{\mathrm{a}=N+1}^{n} \frac{U^2_{\bar{\mathrm{R}}\mathrm{a}}}{\varepsilon - \epsilon_{\mathrm{a}}}, \\ \tilde{u}_{\mathrm{R}}\left(\varepsilon\mathbf{1} - \boldsymbol{\epsilon}_{\mathrm{un}}\right)^{-1} u_{\mathrm{L}} &= \sum_{\mathrm{a}=N+1}^{n} \frac{U_{\bar{\mathrm{R}}\mathrm{a}}U_{\bar{\mathrm{L}}\mathrm{a}}}{\varepsilon - \epsilon_{\mathrm{a}}}, \end{aligned} \tag{52}$$

where $\boldsymbol{\epsilon}_{\mathrm{un}}$ is a diagonal matrix of energies of unoccupied orbitals. These equations encapsulate the essence of Eq. (48), so we define by analogy

$$\begin{aligned} s(\varepsilon) &= \prod_{\mathrm{a}=N+1}^{n} \left(\varepsilon - \epsilon_{\mathrm{a}}\right), \\ \jmath_{\mathrm{pq}} &= s(\varepsilon) \sum_{\mathrm{a}=N+1}^{n} \frac{U_{\mathrm{pa}}U_{\mathrm{qa}}}{\varepsilon - \epsilon_{\mathrm{a}}}. \end{aligned} \tag{53}$$

Provided we are at an energy ε that is away from any molecular eigenvalue $\epsilon_{\rm a}$, we can now simplify the solution of Eq. (41) to give

$$\begin{aligned} C_{\rm L} &= -\frac{\imath N_{\rm L} s}{D}\left(\beta_{\rm R} e^{-\imath q_{\rm R}} - u(\varepsilon)\right), \\ C_{\rm R} &= -\frac{\imath N_{\rm L} s}{D}\jmath(\varepsilon). \end{aligned} \tag{54}$$

The solution for the molecule CI coefficients is

$$C_{\rm a} = (\varepsilon - \epsilon_{\rm a})^{-1}(C_{\rm L}\beta_{\bar{\rm L}{\rm L}}U_{\bar{\rm L}{\rm a}} + C_{\rm R}\beta_{\bar{\rm R}{\rm R}}U_{\bar{\rm R}{\rm a}}). \tag{55}$$

The quantity D can now be expressed as

$$\frac{D}{s} = \left(\beta_{\rm L} e^{-\imath q_{\rm L}} - \frac{t}{s}\right)\left(\beta_{\rm R} e^{-\imath q_{\rm R}} - \frac{u}{s}\right) - \left(\frac{j}{s}\right)^2, \tag{56}$$

so that

$$\begin{aligned} D = \big(&\beta_{\rm L} e^{-\imath q_{\rm L}}\beta_{\rm R} e^{-\imath q_{\rm R}} s \\ &- \beta_{\rm R} e^{-\imath q_{\rm R}} t - \beta_{\rm L} e^{-\imath q_{\rm L}} u + v\big). \end{aligned} \tag{57}$$

It is clear that Eq. (57) looks exactly like Eq. (4). The final expressions for the solutions are

$$\begin{aligned} C_{\rm L} &= -\imath N_{\rm L}\frac{\left(\beta_{\rm R} e^{-\imath q_{\rm R}} s - \beta^2_{\bar{\rm R}{\rm R}} u\right)}{D}, \\ C_{\rm R} &= -\imath \beta_{\bar{\rm L}{\rm L}}\beta_{\bar{\rm R}{\rm R}} N_{\rm L}\frac{\jmath}{D}. \end{aligned} \tag{58}$$

We can now deduce that

$$T = |\tau|^2 = \mathcal{B}(q_{\rm L}, q_{\rm R})\frac{\jmath^2}{|D|^2}. \tag{59}$$

The current flowing through a *configuration function*, $\Psi_0^{a\sigma}$, can be considered as a current flowing through an *orbital* $\psi_{\rm a}\sigma$ with eigenvalue, $\epsilon_{\rm a}$. The expression for this current is

$$\begin{aligned} J_{\rm L\to a} &= \frac{1}{\imath}\left[\langle \Phi_0^{L\sigma} \mid \mathbf{H} \mid \Phi_0^{{\rm a}\sigma}\rangle C^\star_{\rm L} C_{\rm a} - c.c.\right] \\ &= \frac{1}{\imath}\left[\langle \phi_L \mid {\rm h} \mid \psi_{\rm a}\rangle C^\star_{\rm L} C_{\rm a} - c.c.\right] \\ &= \mathcal{B}(q_{\rm L}, q_{\rm R}) U_{\bar{\rm L}{\rm a}} U_{\bar{\rm R}{\rm a}} s_{\rm a}\frac{\jmath}{|D|^2}, \end{aligned} \tag{60}$$

where

$$s_{\rm a} = s/(\varepsilon - \epsilon_{\rm a}) = \prod_{\rm b\neq a}(\varepsilon - \epsilon_{\rm b}) \tag{61}$$

is the polynomial s with an extra eigenvalue excluded from the product. The expression for the orbital current in Eq. 60) is identical to Eq (83) of Pickup *et al.*[17], except for the orbital restrictions implicit in the definitions of the structural polynomials. In cases where orbitals belong to degenerate shells, it is more sensible to discuss shell currents

$$J_{\mathrm{L}\to\mathrm{A}} = \sum_{\mathrm{a}\in\mathrm{A}} J_{\mathrm{L}\to\mathrm{a}} \quad , \tag{62}$$

where A represents a degenerate eigenspace. It is an invariant quantity, *i.e.* its value is independent of the precise choice of MOs inside the shell.

B. Bond currents

We derive expressions for bond currents by noting that the molecule configurations, $\Phi_0^{\mathrm{a}\sigma}$, can be re-expressed using the expansion of the molecular orbitals in terms of atomic orbitals in Eq. (11):

$$\Phi_0^{\mathrm{a}\sigma} = \sum_{\mathrm{p}} \Phi_0^{\mathrm{p}\sigma} U_{\mathrm{pa}}, \tag{63}$$

where, as before,

$$\Phi_0^{\mathrm{p}\sigma} = |\phi_{\mathrm{p}\sigma}\psi_{1\sigma_1}\psi_{2\sigma_2}\cdots\psi_{N\sigma_N}| \tag{64}$$

is a molecular configuration function defined with the occupied MOs *plus* an extra molecular *atomic* orbital ϕ_{p}. Hence, we can re-express the SSP wave-function in Eq. (40) as

$$\Psi^{\mathrm{SSP}} = C_{\mathrm{L}}\Phi_0^{\mathrm{L}\sigma} + \sum_{\mathrm{p}=1}^{n} C_{\mathrm{p}}\Phi_0^{\mathrm{p}\sigma} + C_{\mathrm{R}}\Phi_0^{\mathrm{R}\sigma}. \tag{65}$$

The coefficients, C_{p}, can be derived directly from Eq. (55) using Eq. (63) as

$$\begin{aligned} C_{\mathrm{p}} &= \sum_{a=N+1}^{n} U_{\mathrm{pa}}C_{\mathrm{a}} \\ &= \sum_{a=N+1}^{n} U_{\mathrm{pa}}(\varepsilon-\epsilon_{\mathrm{a}})^{-1}U_{\bar{\mathrm{L}}\mathrm{a}}C_{\mathrm{L}}\beta_{\bar{\mathrm{L}}\mathrm{L}} \\ &+ \sum_{a=N+1}^{n} U_{\mathrm{pa}}(\varepsilon-\epsilon_{\mathrm{a}})^{-1}U_{\bar{\mathrm{R}}\mathrm{a}}C_{\mathrm{R}}\beta_{\bar{\mathrm{R}}\mathrm{R}} \\ &= \hat{\jmath}_{\mathrm{p}\bar{\mathrm{L}}}\beta_{\bar{\mathrm{L}}\mathrm{L}}C_{\mathrm{L}} + \hat{\jmath}_{\mathrm{p}\bar{\mathrm{R}}}\beta_{\bar{\mathrm{R}}\mathrm{R}}C_{\mathrm{R}}. \end{aligned} \tag{66}$$

The last line of this equation is identical to Eq. (63) of Pickup *et al.*,[17] except that we have used the definitions of structural polynomials in terms of virtual MOs (*c.f.* Eq. (53)) appropriate to the many electron molecular state implied by the definitions of the configuration functions in Eqs. (40) and (65). We deduce that the *bond* current is

$$\begin{aligned} J^{\mathrm{bond}}_{\mathrm{p}\rightarrow\mathrm{q}} &= \frac{1}{i}\left(\langle\Phi_0^{\mathrm{p}\sigma}|\hat{H}|\Phi_0^{\mathrm{q}\sigma}\rangle C_{\mathrm{p}}C_{\mathrm{q}} - \mathrm{c.c.}\right) \\ &= -i\beta_{\mathrm{pq}}\left(C_{\mathrm{p}}C_{\mathrm{q}} - \mathrm{c.c.}\right) \\ &= \mathcal{B}(q_{\mathrm{L}}, q_{\mathrm{R}})\beta_{\mathrm{pq}}\frac{\mathcal{J}}{|D|^2}\frac{\mathcal{J}_{\mathrm{p}\bar{\mathrm{L}}}\mathcal{J}_{\mathrm{q}\bar{\mathrm{R}}} - \mathcal{J}_{\mathrm{p}\bar{\mathrm{R}}}\mathcal{J}_{\mathrm{q}\bar{\mathrm{L}}}}{s} \\ &= \mathcal{B}(q_{\mathrm{L}}, q_{\mathrm{R}})\beta_{\mathrm{pq}}\frac{\mathcal{J}}{|D|^2}v_{\mathrm{pq}\bar{\mathrm{L}}\bar{\mathrm{R}}}, \end{aligned} \tag{67}$$

where the quantity $v_{\mathrm{pq}\bar{\mathrm{L}}\bar{\mathrm{R}}}$ is defined by

$$v_{\mathrm{pq}\bar{\mathrm{L}}\bar{\mathrm{R}}} = \frac{\mathcal{J}_{\mathrm{p}\bar{\mathrm{L}}}\mathcal{J}_{\mathrm{q}\bar{\mathrm{R}}} - \mathcal{J}_{\mathrm{p}\bar{\mathrm{R}}}\mathcal{J}_{\mathrm{q}\bar{\mathrm{L}}}}{s}, \tag{68}$$

using a more general version of the Jacobi-Sylvester relation[14] as given by Brualdi *et al.*[38]

The set of functions, $\{\Phi^{\mathrm{p}\sigma}\}$, used in this derivation of bond currents is over-complete and non-orthogonal. The expression for Ψ^{SSP} in Eq. (65), however, has two essential ingredients required to derive bond currents. First, it contains the core of occupied molecular orbitals in each configuration function. Secondly, it has a set of configurations describing an extra electron passing through the molecule defined in terms of the atomic orbitals required for a definition of a bond current.

The SSP wave-function in Eq. (65) can be used to derive secular equations analogous to Eq. (41) and (42), but the non-orthogonality of the configuration functions requires the use of Löwdin rules for the simplification of CI matrix elements. This derivation and solution of the equations is a long-winded alternative, but ultimately yields the same result.

At this point, we have explicit expressions for total current and bond current when Pauli exclusion is taken into account. These can be used directly to calculate $T(\varepsilon)$ and map out conduction pathways in individual cases. The central advantage of a graph theoretical approach is that it predicts generic features of conduction, embodied in selection rules. To explore these in the new model requires investigation of some properties of the modified structural polynomials.

IV. CONSEQUENCES FOR CONDUCTION BEHAVIOUR AND SELECTION RULES

The selection rules for conduction derived previously[15,17,39] depend crucially on the interlacing properties of the four structural polynomials. In the present section we first check that these properties are retained by the modified structural polynomials (section IV A) and then give the selection rules in the form that applies to the new model (section IV B).

A. Interlacing properties of structural polynomials

In adopting the definition of the structural polynomials in Eq. (53), we have lost the equivalence of the original structural polynomials[17] to characteristic polynomials of vertex-deleted graphs, but have retained their form as sums over states of the molecule, at the price of simple deletions of a set of occupied orbitals from the sums. As noted above, this is effectively a projection of spectral representations into the space of unoccupied molecular orbitals.

In order to use the new interpretation of the equations to derive the behaviour of transmission at specific energies, we need to be confident that these restricted polynomials obey the same *selection rules*. The selection rules were originally derived using the interlacing properties of the original polynomials s, t, u, and v, which follow from their relationship to vertex-deleted versions of the original graph. Roots of t (and u) interlace those of s, and the roots of v interlace those of t, and u.[40] It is not obvious that the new polynomials have these same properties. However, the new t and u can be understood through their spectral definitions

$$\hat{t} = t/s = \sum_{a} \frac{U_{\mathrm{a}\bar{\mathrm{L}}}^2}{\varepsilon - \epsilon_{\mathrm{a}}}$$

$$\hat{u} = u/s = \sum_{a} \frac{U_{\mathrm{a}\bar{\mathrm{R}}}^2}{\varepsilon - \epsilon_{\mathrm{a}}} \tag{69}$$

which imply non-positive gradients

$$\frac{dt}{d\varepsilon} \leq 0, \quad \frac{du}{d\varepsilon} \leq 0. \tag{70}$$

The zeros of the hatted polynomials in Eq. (69) are just the roots of t and u, respectively, and so the interlacing properties of the roots of these quantities with the roots of s follow directly. Interlacing properties of s, t, and u are given more formally by Lemma 1.20 on page 13 of the book by Fiske.[41]

Interlacing of the roots of v with those of t and u follows from the argument below. The Jacobi-Sylvester relation in Eq (7) is equivalent to

$$\hat{v}(\varepsilon) = v/s = \hat{u}\hat{t} - \hat{\jmath}^2. \tag{71}$$

We can look at the behaviour of $\hat{v}$ at the zeros ϵ_t of $\hat{t}$. It follows from the preceding equation that

$$\hat{v}(\epsilon_t) = \hat{u}(\epsilon_t)\hat{t}(\epsilon_t) - \hat{\jmath}(\epsilon_t)^2 = -\hat{\jmath}(\epsilon_t)^2 \le 0, \tag{72}$$

for all roots ϵ_t. Consider, for simplicity, a case where the roots of s are non-degenerate. Using the interlacing properties of the roots of s and t, we can write

$$\cdots \le \epsilon_a \le \epsilon_t \le \epsilon_{a+1} \le \epsilon_{t+1} \le \cdots \tag{73}$$

It is clear that in the expression

$$s(\epsilon) = (\epsilon - \epsilon_{\mathrm{a}})\,(\epsilon - \epsilon_{\mathrm{a+1}}) \prod_{\mathrm{b<a}} (\epsilon - \epsilon_{\mathrm{b}}) \prod_{\mathrm{b>a+1}} (\epsilon - \epsilon_{\mathrm{b}}) \tag{74}$$

the terms in the two extended products have the same sign when $\epsilon = \epsilon_t$, and when $\epsilon = \epsilon_{t+1}$. The first two terms, on the other hand, are overall negative for $s(\epsilon_t)$, and positive for $s(\epsilon_{t+1})$. It follows that $s(\epsilon)$ changes sign over the interval $\epsilon_t \le \epsilon \le \epsilon_{t+1}$. The implication is that the function

$$v(\epsilon) = s(\epsilon)\hat{v}(\epsilon)$$

changes sign in that interval, and that there is a root of v between any two roots of t. An identical argument proves that the roots of v interlace the roots of u.

We now see that the four structural polynomials defined in terms of the restricted set of unoccupied one-electron states share all the properties of their unrestricted analogues.[17]

B. Conduction cases for *ipso* and *non-ipso* molecular devices

The results derived thus far are for the total transmission, and for currents at values of ε away from any unoccupied eigenvalue. We can investigate the behaviour of these quantities at eigenvalues by expanding them in Laurent series and taking limits, exactly as shown in Pickup *et al.*.[17] We do not need to repeat the analysis here.

Kind	r_{A}	Case	g_t	g_u	g_v	g_j	$T\,(\epsilon_{\mathrm{A}})$	$J^{\mathrm{bond}}_{\mathrm{p}\to\mathrm{q}}(\epsilon_{\mathrm{A}})$	$J_{\mathrm{L}\to\mathrm{A}}(\varepsilon)$
Two CFVs	0	1	$g{+}1$	$g{+}1$	$g{+}2$	$\geq g{+}1$	0	0	0
	0	2	$g{+}1$	$g{+}1$	g	g	$\neq 0$	$\neq 0$	0
	0	3	$g{+}1$	g	$g{+}1$	$\geq g{+}1$	0	0	0
	0	4	$g{+}1$	g	g	g	$\neq 0$	$\neq 0$	0
	0	6	g	g	$g{+}1$	g	$\neq 0$	$\neq 0$	0
	0	7.1	g	g	g	g	$\neq 0$	$\neq 0$	0
	0	7.2	g	g	g	$\geq g{+}1$	0	0	0
CV and CFV	1	5	$g{+}1$	$g{-}1$	g	$\geq g$	0	0	0
	1	8	g	$g{-}1$	$g{-}1$	$\geq g$	0	0	0
Two CVs	1	9	$g{-}1$	$g{-}1$	g	$g{-}1$	$\neq 0$	$\neq 0$	$\neq 0$
	1	10	$g{-}1$	$g{-}1$	$g{-}1$	$g{-}1$	$\neq 0$	$\neq 0$	$\neq 0$
	2	11.1	$g{-}1$	$g{-}1$	$g{-}2$	$g{-}1$	0	0	$\neq 0$
	2	11.2	$g{-}1$	$g{-}1$	$g{-}2$	$\geq g$	0	0	0
–	–	PSB	–	–	–	–	0	0	0
≥ 1 CFV	0/1	PPR	–	–	–	–	0	0	0

TABLE I. Conduction cases for *non-ipso* molecular devices, showing the kind of the vertex pair for the device, the *rank* of the connection matrix r_{A} for shell A with eigenvalue ϵ_{A} and degeneracy g, the total transmission $T\,(\epsilon_{\mathrm{A}})$, and the bond currents $J^{\mathrm{AO}}_{\mathrm{p}\to\mathrm{q}}(\epsilon_{\mathrm{A}})$. The numbers of repeated roots in structural polynomials, t, u, v, and j are g_t, g_u, g_v, and g_j, respectively. The shell current $J_{\mathrm{L}\to\mathrm{A}}(\varepsilon)$ applies for *any* energy. CV and CFV stand respectively for core and core-forbidden vertices (defined with respect to the eigenspace A). Case PSB is Pauli Spin Blockade. Case PPR (Pauli Perfect Reflector) occurs when the structural polynomial $\jmath(\varepsilon)$ is zero for all values of ε.

The classification of conduction/insulation cases for *non-ipso* devices is shown in Table I, and for *ipso* devices in Table II. The tables give information about conduction or insulation (in terms of the total transmission and bond currents) when the incoming electron energy, ε, coincides with a molecular eigenvalue. They also give information about the shell current (at *any* energy) for the shell belonging to that eigenvalue.

The cases are classified by the rank of the matrix block in the SSP equations that describes the connection from source and sink to the molecule, and also by the nature of the graph vertices representing the link atoms $\bar{\mathrm{L}}$ and $\bar{\mathrm{R}}$. There are two categories of vertex: core (CV) and core-forbidden(CFV). A core-forbidden vertex (with, say index p) for an eigenspace (shell) with eigenvalue ϵ_{A} has $U_{\mathrm{pa}} = 0$, for all a $\in$ A. Core vertices are just those vertices that are not core-forbidden. Terms CV and CFV are normally used for the case with $\epsilon_{\mathrm{A}} = 0$, but here we allow the classification of a vertex to be specified for each eigenspace.

The cases are further subdivided by the behaviour of the structural polynomials t, u, and v, in terms of multiplicities of the specific eigenvalue. There are 11 cases for *non-ipso* devices as shown in Table I. The polynomial $\jmath$ shows more complex behaviour, because it is not constrained by interlacing. Some cases (2, 4, 6, 9, and 10) have their g_j root behaviour determined exactly through relationships dictated by the Jacobi-Sylvester relation shown in Eq. (7). In the remaining cases (1, 3, 7, 5, 8, and 11), the Jacobi-Sylvester relation dictates only a minimum value of g_j. This behaviour makes a difference to the prediction transmission only in cases 7 and 11, where we distinguish sub-cases. In the others, an increase in $g_\jmath$ does not affect conduction or insulation. It does, however, affect the shape of the dip in transmission at the eigenvalue. There are many small molecules where these effects may be seen in the predicted transmission curve.

The *ipso* connection exhibits simpler behaviour, as there is only a single connection site ($\bar{\mathrm{L}} = \bar{\mathrm{R}}$) and a single structural polynomial t. If the connection site is a CFV (a rank 0 connection matrix for the shell), g_t is limited by interlacing to two possible values, namely $g + 1$, or g. Connection via a CV requires $g_t = g$. Hence there are just three *ipso* cases.

In both tables we have added two additional cases: 'PSB', which is the insulating Pauli Spin Blockade, and 'PPR ', which is Pauli Perfect Reflection. These are described in the next section.

Kind	$r_{\rm A}$	Case	g_t	$T\,(\epsilon_{\rm A})$	$J^{\rm bond}_{\rm p\to q}(\epsilon_{\rm A})$	$J_{\rm L\to A}(\varepsilon)$
CFV	0	I1	$g{+}1$	0	0	0
		I2	g	$\neq 0$	0	0
CV	1	I3	$g{-}1$	$\neq 0$	0	$\neq 0$
–	–	PSB	–	0	0	0
CFV	0	PPR	–	0	0	0

TABLE II. Conduction cases for *ipso* molecular devices, showing the kind of the vertex pair for the device, the *rank* of the connection matrix $r_{\rm A}$ for shell A with eigenvalue $\epsilon_{\rm A}$ and degeneracy g, the total transmission $T\,(\epsilon_{\rm A})$, and the bond currents $J^{\rm AO}_{\rm p\to q}(\epsilon_{\rm A})$. The number of repeated roots in the structural polynomial, t, is g_t. CV and CFV stand respectively for core and core-forbidden vertices (defined with respect to the eigenspace with eigenvalue $\epsilon_{\rm A}$). The shell current $J_{\rm L\to A}(\varepsilon)$ applies for *any* energy. Case PSB is Pauli Spin Blockade. Case PPR (Pauli Perfect Reflector) occurs when the structural polynomial $\jmath(\varepsilon)$ is zero for all values of ε.

V. BEHAVIOUR ARISING FROM THE MOLECULAR ELECTRONS

The presence of a space of occupied spin-orbitals with the same spin as the scattering electron introduces new behaviour in three different ways.

A. Pauli Spin Blockade

The first effect arises because only virtual spin-orbitals with spin σ appear in the SSP equations. Occupied orbitals, and orbitals of opposite spin to the scattering electron do not appear at all. It follows that there can be no shell currents involving these orbitals for any connection pattern and for any energy ε. We refer to this situation as Pauli Spin Blockade (case PSB) in tables I and II.

A natural outcome of inclusion of Pauli effects in the Hückel/SSP formalism is the removal of transmission peaks at energies below the molecular Fermi level. Occupation of molecular spin-orbitals removes energy levels from consideration in the all-important structural polynomials. Transmission below the Fermi energy is not removed altogether, but the curve typically tails off smoothly towards to the low energy side of the first active shell.

B. Pauli Perfect Reflection

There is a second consequence of inclusion of Fermi statistics: at certain orbital occupancies for certain molecules, conduction is suppressed for *all* energies; systems can become *Pauli Perfect Reflectors* (case PPR in Tables I and II).

The rationale for this claim is as follows. The form of the structural polynomial $\hat{\jmath}_{\bar{\mathrm{L}},\bar{\mathrm{R}}}$ is

$$\hat{\jmath}_{\bar{\mathrm{L}}\bar{\mathrm{R}}} = \sum_{\mathrm{A}} \sum_{a\in\mathrm{A}} U_{\bar{\mathrm{L}}\mathrm{a}} U_{\bar{\mathrm{R}}\mathrm{a}}/(\varepsilon - \epsilon_{\mathrm{a}}), \tag{75}$$

where the sum runs over eigenspaces A from LUMO (lowest unoccupied molecular orbital) to HUMO (highest unoccupied molecular orbital). (We allow only Hund's Rule configurations, so every shell is filled, half-filled with all electrons of the same spin, or empty.) If the sum

$$\sum_{a\in\mathrm{A}} U_{\bar{\mathrm{L}}\mathrm{a}} U_{\bar{\mathrm{R}}\mathrm{a}}$$

vanishes for every eigenspace A included in the spectral representation of $\hat{\jmath}$ for electrons of spin σ, the device with connection vertices $\bar{\mathrm{L}}, \bar{\mathrm{R}}$ in molecular graph G will be a perfect reflector for incoming electrons of that spin, with $T_\sigma(\varepsilon) = 0$ for *all* ε in the range of wire energies. If the molecule has a closed shell within the model, then conduction of electrons of both spins will be blocked at all energies.

Vanishing of $\hat{\jmath}$ may seem to be a strong or even outrageous requirement, but in fact it is met for many shells of many small chemical graphs. We need only that either $\bar{\mathrm{L}}$ or $\bar{\mathrm{R}}$ or both will be a CFV in each of the unoccupied shells; this can often be arranged by selecting shells with particular symmetries. Hundreds of molecular graphs for which the HUMO-shell has CFVs are found by simple search of chemical graphs with $5 \leq n \leq 14$, for example.

Construction of a case of PPR based on such graphs solely on Aufbau electronic configurations, *i.e.*, where all occupied spin-orbitals have lower energy than all unoccupied spin-orbitals of the same spin, often leads to implausibly high molecular charges, but Pauli Perfect Reflection is also predicted for *excited states*, which could be achieved by, for example, photo-excitation.

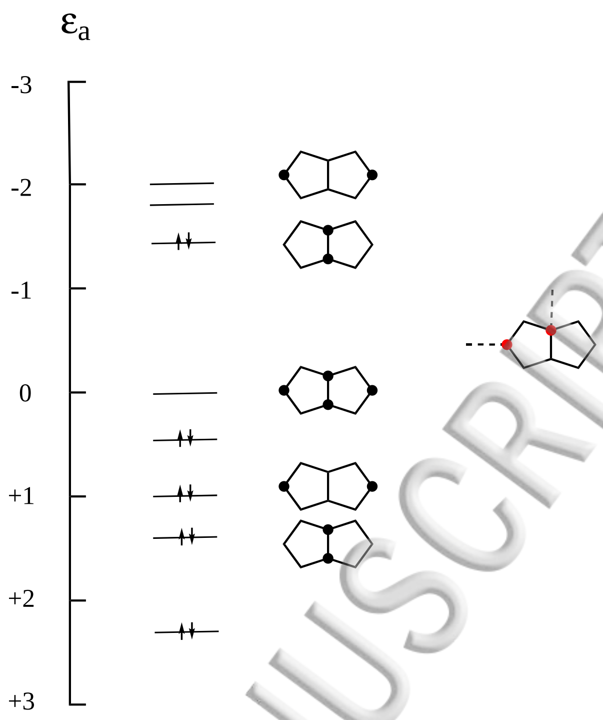

FIG. 2. Pauli Perfect Reflection in devices based on pentalene. The pentalene molecular graph has characteristic polynomial $s = \varepsilon(\varepsilon - 1)(\varepsilon + 2)(\varepsilon^2 - 2)(\varepsilon^3 - \varepsilon^2 - 4\varepsilon + 2)$, which gives the spectrum shown on the left. All eigenvectors except the three corresponding to the irreducible factor of s have CFVs (as shown with black dots in the diagram). The 10π excited configuration of the dianion connected as shown by the red dots, is therefore a Pauli Perfect Reflector, with $\hat{t}^{-1} = 4(\varepsilon + 2)$, $\hat{u}^{-1} = 3(\varepsilon + \sqrt{2})$, $\hat{v} = \hat{u}\hat{t}$, and $\hat{\jmath} = 0$.

A small chemical example of this type based on pentalene is shown in Fig. 2. The molecular graph of pentalene has eight eigenvectors, five of which have CFVs, in positions determined by the mirror planes of the point group, as illustrated in the figure. As a consequence, the only transmission predicted for a device based on the neutral pentalene molecule and with one connection in each mirror plane (as shown in red in the figure) is *via* the highly antibonding shell 7. However, excitation of the pentalene molecular dianion into the configuration illustrated in the figure would give $T(\varepsilon) = 0$, and hence perfect reflection. Many other examples can be constructed.

C. Case migration

There is a third, more technical, effect arising from the presence of the molecular electrons, and that is migration between selection-rule cases as electronic occupation increases. When a shell is removed from the sums that define the polynomials s, t, u and v, the multiplicity of a root corresponding to another eigenvalue may change. The allowed changes of case are limited by the fact that the rank is a property of the shell independently of occupation of other shells. Other shell invariants include the leading terms in the Laurent expansions of the structural polynomials around the shell eigenvalue.[17] Detailed considerations of this kind lead to the following 'propensity rules'. For rank 2, cases 11.1 and 11.2 cannot exchange. For rank 1, insulating cases 5 and 8 may exchange, as can conducting cases 9 and 10. For rank 0, various exchanges are possible, including conversions from insulating to conducting cases. Conversion to case 7.1 is common, for example. A shell may change case several times before its own occupation by electrons ultimately removes it from the SSP equations.

VI. EXAMPLES

We show results calculated from the equations presented above, using the computer-algebra package Maple.[42] All calculations have been carried out with Hückel parameters $\alpha = \alpha_{\mathrm{L}} = \alpha_{\mathrm{R}} = 0$, $\beta_{\mathrm{L}} = \beta_{\mathrm{R}} = 1.4\beta$, and all energies are in units of β. The consequence is that occupied orbitals (positive values of β/ε) are shown on the left of the figures below, and unoccupied orbitals on the right. With these parameters, this is a zero-bias device with conduction bands for the leads that are wide enough to access all molecular states.

A. The five-membered chain

Results are shown in Fig. 3 for a five-membered chain, with the source and sink atoms connected to terminal atoms.

The upper panel shows conduction in the hypothetical case of the molecule with all molecular-orbital channels open, which is formally equivalent to a calculation in which N, the number of electrons in the molecule, is set to zero. It has five peaks in transmission corresponding to the five non-degenerate orbitals (= shells). Each orbital provides a channel for conduction, such that the total transmission at electron energy ε is the sum of the currents

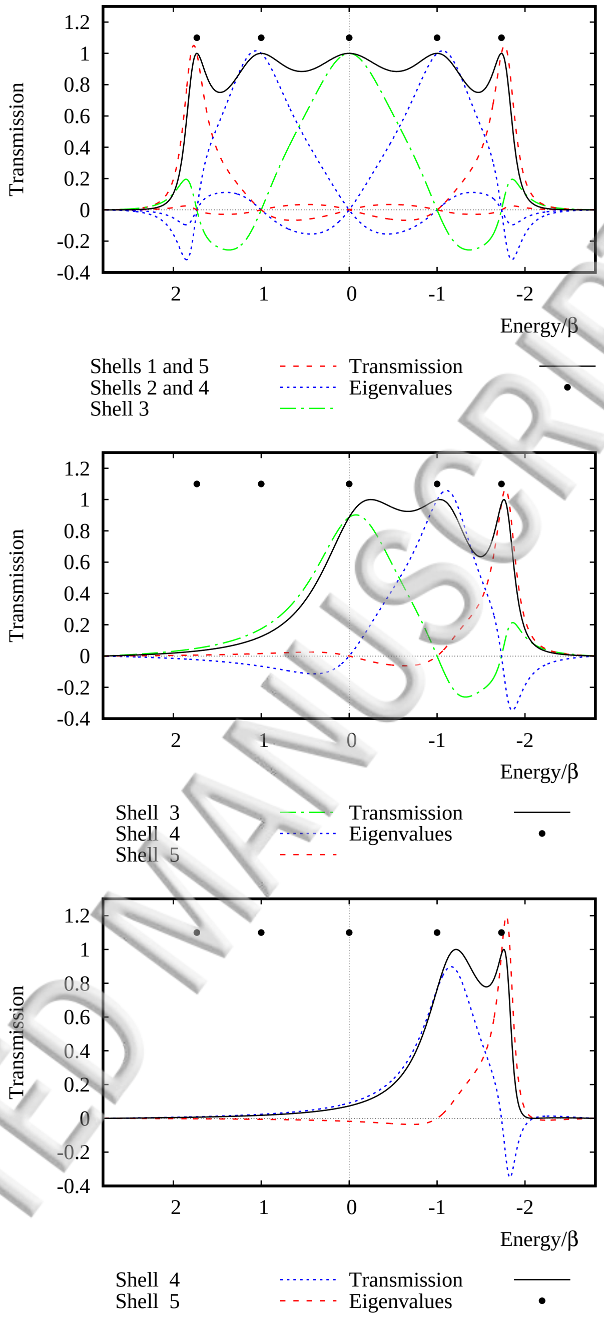

FIG. 3. A five-membered chain with terminal connections to source and sink. Upper, middle, and lower diagrams show transmission and shell currents for the device with 0, 2, and 3 molecular electrons having the same spin as the incoming electron. Orbital energies are shown for reference as black circles above the curves.

passing through the individual orbitals. In this example, all current passes through a *single* orbital when the input electron stream has an energy equal to the eigenvalue of that orbital. Individual orbitals have zero conduction at eigenvalues other than their own.

The middle panel shows the conduction pattern when the molecule has a ground-state of four spin-paired electrons in the lowest two orbitals. The peaks from shells 1 and 2 are missing, and are examples of Pauli Spin Blockade. Conduction can occur only through empty orbitals 3, 4, and 6. We emphasise, however, that there is still some conduction through the virtual orbitals at energies below the Fermi energy. The exclusion principle closes shells occupied by electrons of spin σ to conduction electrons of that spin. If we assume that the ground-state of the π-system has five electrons, comprising two pairs in MOs 1 and 2, and a single α-spin electron in orbital 3, then this diagram would describe the conduction of a β-spin electron down the left-hand wire. Such an electron would not be excluded from passing through orbital 3. The passage of an electron of α-spin, however, would be excluded from this orbital, and therefore the bottom panel would be an appropriate description for α-spin conduction. Naturally, one would have to sum up appropriately the diagrams to get overall transmission, if neither the spin of the molecular state, nor that of the incoming electron, is selected.

Note that orbital/shell currents can be negative, or can exceed unity, whereas $0 \leq T_\sigma(\varepsilon) \leq 1$. Individual shell currents of active shells vary, if sometimes only slightly, with occupation of other shells. In the present simple example, all orbitals are conducting (case 10) and active. Orbital 5 is case 9 which is also conducting and active. Orbital 5 changes to case 10 in the middle panel (*c.f.* section V).

B. Anthracene in a symmetrical *non-ipso* device

Shell currents for an anthracene-based device with source and sink atoms connected to the central apical atoms, are shown in Fig. 4. The point group of anthracene is D_{2h}, and the shell currents reflect this symmetry. In particular shells 2, 4, 7 and 9 have a node on the central apical atoms that renders them inert to conduction. The transmission profile has peaks corresponding to the six shells that are symmetric with respect to the mirror plane through the connection atoms (*c.f.* table III).

The lower panel of the figure shows the conduction pattern for a molecule with a 14-

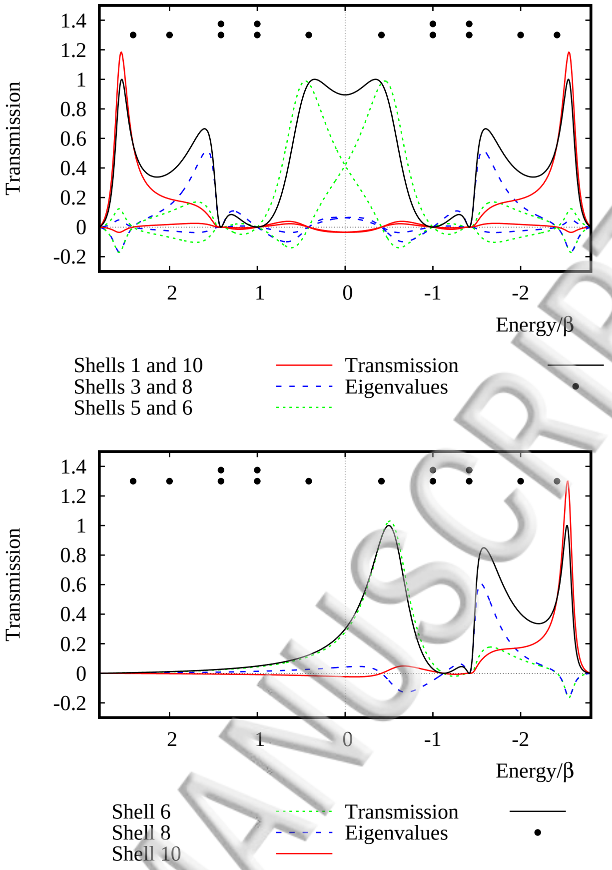

FIG. 4. Anthracene with central apical atoms connected to source and sink. The upper diagram shows the transmission for a molecule with all channels open, and the lower diagram shows the transmission for the 14 electron ground-state.

electron ground-state (*i.e.* seven orbitals occupied by a pair of electrons). The three peaks represent transmission through the remaining three unoccupied *symmetrical* MOs. The detailed cases for the shells are not necessarily constant as orbital occupancy changes, as noted in section V. An example of this is shell 7 which migrates to case 7.1, and shell 9 which changes from case 6 to 7.1.

The closed-shell ground-state implies that there will be no difference in transmission for an α- or a β-spin electron. One would need still need to sum over both possibilities to get the total transmission for an unpolarised stream of electrons.

The bond currents in Fig. 5 also reflect the existence of peaks in the overall transmission, six for $N = 0$, and three for $N = 14$. Note that currents through particular orbitals may be *negative*, but currents through available bond paths must sum to the total transmission. The bond currents shown represent only two of the four paths that would contribute to the

Shell	Symmetry	Eigenvalue	Case(0)	Case(14)
1	A_g	$1+\sqrt{2}$	10	PSB
2	B_{3u}	2	6	PSB
3	$A_g + B_{2u}$	$\sqrt{2}$	11.1	PSB
4	$B_{1g} + B_{3u}$	1	1	PSB
5	B_{2u}	$-1+\sqrt{2}$	10	PSB
6	B_{2u}	$1-\sqrt{2}$	10	10
7	$B_{1g} + B_{3u}$	-1	1	7.1
8	$A_g + B_{2u}$	$-\sqrt{2}$	11.1	11.1
9	B_{3u}	-2	6	7.1
10	A_g	$-1-\sqrt{2}$	10	10

TABLE III. Conduction cases at the molecular eigenvalues (in units of β) of anthracene for two different electron occupancies. Case(0) and Case(7) are the cases for molecular electron counts of 0 (i.e., all channels open) and 14, respectively. The device is formed by connections to atoms at apical points of the middle ring. Shells 1 to 5 are insulating for 14-electron ground-states because of Pauli Spin Blockade. Shells 2, 4, 7 and 9, are inert for all ground-states owing to their antisymmetry with respect to the vertical mirror plane through connection atoms.

total current for anthracene.

C. Anthracene in a symmetrical *ipso* device

Ipso devices have source and sink linked to the same atom in the molecule. In this case we have chosen a central apical atom through which the mirror plane passes. The hypothetical $N = 0$ example in the upper panel of Fig. 6 shows the six peaks we expect, owing to mirror symmetry. The lower panel shows the transmission for the molecular ground-state ($N = 14$), where again, the occupied orbitals show the effects of Pauli Spin Blockade. There are no bond currents for *ipso* devices, as no currents pass through the molecular framework. The MOs,

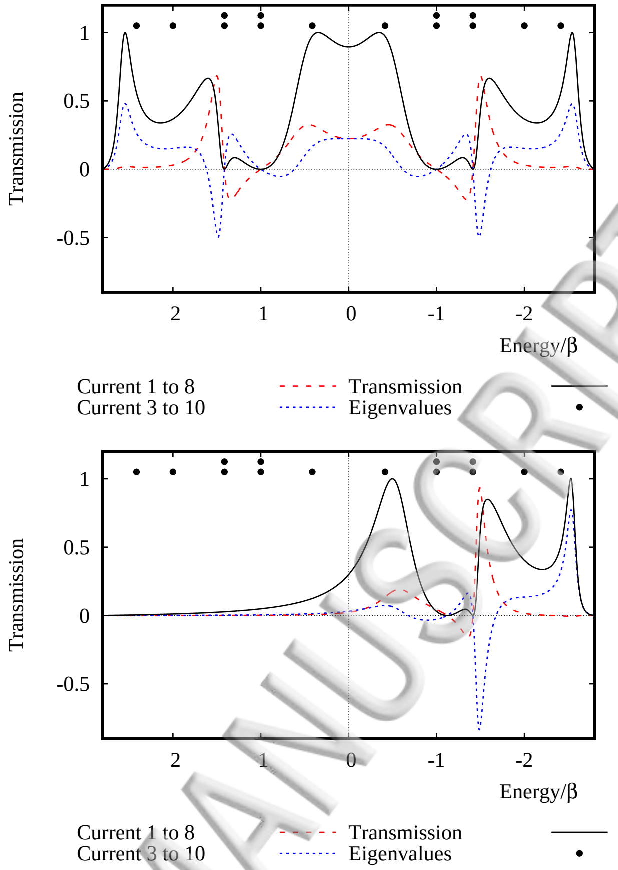

FIG. 5. Anthracene transmission and bond currents with central apical atoms connected to source and sink. The upper diagram is for a molecule with all channels open, equivalent to $N = 0$, and the lower diagram is for the molecule with a 14-electron ground-state. The currents in edges 1 to 8 and 3 to 10 are, respectively, in the leftmost and rightmost edge of an end hexagon of anthracene, both taken in a direction towards the sink connection atom.

however, transfer current from source to sink, depending on the vanishing, or otherwise, of MO coefficients on the connection atom. The $N = 0$ example shows insulation at $\varepsilon = 0$, whereas the molecular ground state shows a sizeable transmission. The $\jmath$ polynomial has a root at $\varepsilon = 0$ causing insulation in the one-electron model, whereas the removal of half the orbitals contributing to $\jmath$ for the many-electron case suppresses this root.

VII. CONCLUSION

We have derived a consistent formalism for ballistic conduction that includes Fermi statistics in the SSP model at the Hückel level of treatment. It turns out that the new formalism

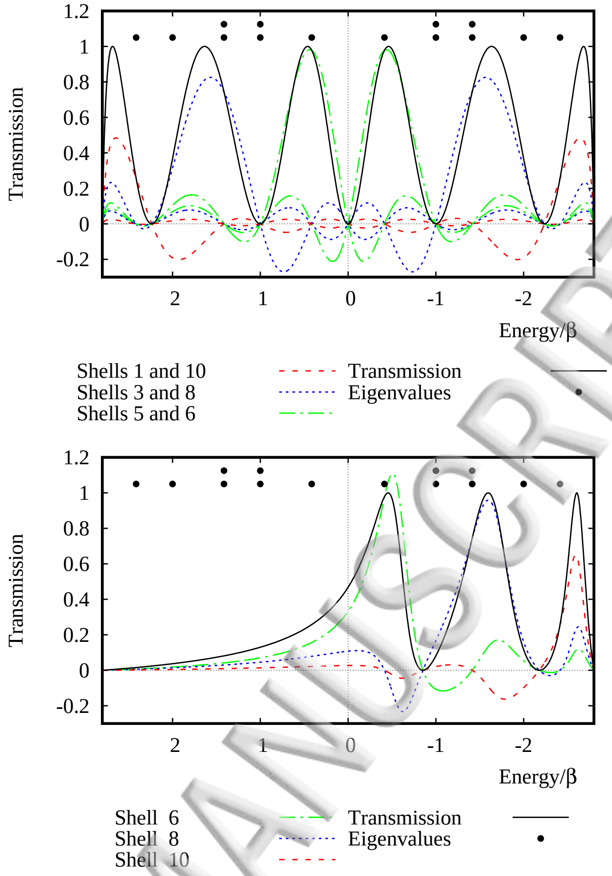

FIG. 6. Anthracene transmission and shell currents for an *ipso* device with a single central apical atom connected to source and sink. The upper diagram is for a molecule with all channels open, and the lower diagram shows is for the molecule with a 14-electron ground-state.

maps exactly onto the previous Hückel-SSP model[17], in which electron interaction was neglected. The conversion is achieved by changing some definitions: in the new formalism, all structural polynomials are projected onto the space of unoccupied orbitals.

In this version of the SSP model, the device wave-function is generated from a 'source' configuration function (determinant), representing a single electron of fixed spin on the source atom, and a product of spin-orbitals occupied in the molecule. This source configuration is a fixed eigenfunction of the S_z operator with some eigenvalue M_S. The device wave-function comprises a limited set of configuration functions formed from a set of single excitations derived by allowing the source electron to progress through the unoccupied orbitals of the molecule from source into sink. The tight-binding approximation does not include the effects of electron correlation, and so the energies of all states corresponding to a given orbital occupancy are equal, irrespective of the spin, within this model.

The z-component of spin is relevant in so far as it dictates which configurations will interact. The situation is different as soon as there is two-electron interaction, such as that in the Hubbard Hamiltonian,[30,43] or in more complicated cases, such as the PPP Hamiltonian[44,45]. In such a case, singlets and triplets with the same orbital occupancy will differ in energy. In addition, more configuration functions, beyond single excitations, will contribute to the expression for the device wave-function. One method for incorporating electron-electron interactions that uses parametrised electron repulsion and correlation is the scattering approach described by Subotnik and Nitzan.[34]

The present Hückel/Pauli/SSP model gives information about orbital (shell) and bond currents, which are both valuable from the point of view of interpretation. This is made possible *solely* because the molecular configuration functions contain a single electron in an unoccupied MO (or AO for bond currents), allowing them to be identified by that orbital. In models that include electron-electron interactions, and that couple higher excitations, this will no longer be possible.

Even within the Hückel approximation, there may be a need to sum over different spin orientations to obtain a total transmission. It is also possible that other channels for scattering may be available within the energy range dictated by the width of the bands in the wires. One possibility is that an electron from the highest occupied level of the molecule could hop into the sink. This scenario suggests that there might be conduction using an N-electron model, as opposed to the $(N+1)$-electron version we have used in this paper. The electron removed from the molecule could then be replaced by an electron appearing on the source, and hopping onto the molecule. Ernzerhof[29] has based his model of correlation effects on conduction on a model of this sort, although much of his emphasis is upon the effects of two-electron interactions *via* the introduction of a Hubbard potential between the electrons. The present model recovers Ernzerhof's results[29] for $T(E)$ in the limit of a zero Hubbard interaction; this is simply achieved by subtracting one from the count of molecular electrons with the same spin as the incoming electron. The transmission curves in this case will show extra structure at energies below the Fermi level compared to $T(E)$ in the present approach. As discussed in Ref 29, such structure may indicate an exaggeration of the effects of electron occupancy.

All of these possible scattering channels are uncoupled in the tight-binding model, and all such channels that are energetically available must be summed to provide a full understanding of molecular conduction. In particular, subtle effects such as the collapse[18] and even reversal[20] of Pauli Spin Blockade are explained by the opening of new channels as their energies are tuned by external fields. We note that the tight-binding SSP approach used in the present paper can easily be extended to admit external fields, such as an applied electric or magnetic field; electric fields can be included by modifying diagonal terms in the Hamiltonian,[46,47] and magnetic fields by use of a London modification of the off-diagonal terms. Hyperfine terms that change the spin can also be included in phenomenological Hamiltonians of the tight-binding form. Such extensions to the model could predict, for example, molecular analogues of the significant changes in transmission with magnetisation that have been observed in spin-polarised STM experiments.[31,33]

Finally, it should be noted that the Hückel-SSP model with Fermi statistics remains resolutely graph-theoretical. In order to calculate device transmission as a function of electron energy within this approach, all that is required is the molecular graph, an identification of connection vertices and a molecular electron count. Diagonalisation of the adjacency matrix gives the rest. The nature of the model is that it can give predictions of global types of behaviour for classes of molecular conductors, as we have seen here with the examples of Pauli Spin Blockade and Pauli Perfect Reflection, acting as a complement to more sophisticated calculations on specific systems.

REFERENCES

[1] A. Aviram and M. A. Ratner, Chem. Phys. Lett. **29**, 277 (1974).
[2] A. Nitzam, Ann. Rev. Phys. Chem. **52**, 681 (2001).
[3] M. A. Ratner, Nature Nanotechnology **8**, 378 (2013).
[4] R. M. Metzger, Chemical Reviews **115**, 5056 (2015).
[5] L. Sun, Y. A. Diaz-Fernandez, T. A. Gschneidtner, F. Westerlund, S. Lara-Avila, and K. Moth-Poulsen, Chemical Society Reviews **43**, 7378 (2014).
[6] R. M. Metzger and D. L. Mattern, Topics in Current Chemistry **313**, 39 (2012).
[7] Nature Nanotechnology, Molecular Electronics Focus Issue, Vol. 8 (Springer Nature, 2013) pp. 377–467.
[8] *Organic Photonics and Electronics*, Faraday Discussions (The Royal Society of Chemistry, 2015).

[9] D. M. Guldi, H. Nishihara, and L. Venkataraman, Chem. Soc. Rev. **44**, 842 (2015).

[10] J. C. Cuevas and E. Scheer, *Molecular Electronics: An Introduction to Theory and Experiment* (World Scientific, Singapore, 2010).

[11] K. Moth-Poulsen, *Handbook of Single-Molecule Electronics* (CRC, Boca Raton, FL, 2015).

[12] F. Goyer, M. Ernzerhof, and M. Zhuang, J. Chem. Phys. **126**, 144104 (2007).

[13] B. T. Pickup and P. W. Fowler, Chem. Phys. Lett. **459**, 198 (2008).

[14] J. J. Sylvester, Philos. Mag. **1**, 295 (1851).

[15] P. W. Fowler, B. T. Pickup, T. Z. Todorova, and W. Myrvold, J. Chem. Phys. **131**, 044104 (2009).

[16] I. Sciriha, M. Debono, M. Borg, P. W. Fowler, and B. T. Pickup, Ars Mathematica Contemporeana **6**, 261 (2013).

[17] B. T. Pickup, P. W. Fowler, M. Borg, and I. Sciriha, J. Chem. Phys. **143**, 194105 (2015).

[18] K. Ono, D. Austing, Y. Tokura, and S. Tarucha, Science **297**, 1313 (2002).

[19] T. Kodera, K. Ono, S. Amaha, Y. Arakawa, and S. Tarucha, Journal of Physics: Conference Series **150**, 022043 (2009).

[20] J. K. Perron, M. D. Stewart, and N. M. Zimmerman, J. Appl. Phys. **119**, 134307 (2016).

[21] J. R. Petta, A. C. Johnson, A. Yacoby, C. M. Marcus, M. P. Hanson, and A. C. Gossard, Phys. Rev. B **72**, 161301 (2015).

[22] Y. Hu, F. Kuemmeth, C. M. Lieber, and C. M. Marcus, Nat. Nano. **7**, 47 (2012).

[23] A. C. Johnson, J. R. Petta, J. M. Taylor, A. Yacoby, M. D. Lukin, C. M. Marcus, M. P. Hanson, and A. C. Gossard, Nature **435**, 925 (2005).

[24] S. Nadj-Perge, S. M. Frolov, J. W. W. van Tilburg, J. Danon, Y. V. Nazarov, R. Algra, E. P. A. M. Bakkers, and L. P. Kouwenhoven, Phys. Rev. B **81**, 201305 (2010).

[25] J. R. Petta, A. C. Johnson, J. M. Taylor, E. A. Laird, A. Yacoby, M. D. Lukin, C. M. Marcus, M. P. Hanson, and A. C. Gossard, Science **309**, 2180 (2005).

[26] F. H. L. Koppens, C. Buizert, K. J. Tielrooij, I. T. Vink, K. C. Nowack, T. Meunier, L. P. Kouwenhoven, and L. M. K. Vandersypen, Nature **442**, 766 (2006).

[27] K. C. Nowack, F. H. L. Koppens, Y. V. Nazarov, and L. M. K. Vandersypen, Science **318**, 1430 (2007).

[28] A. Goker, F. Goyer, and M. Ernzerhof, J. Chem. Phys. **129**, 194901 (2008).

[29] F. Goyer and M. Ernzerhof, J. Chem. Phys. **134**, 174101 (2011).

[30] J. Hubbard, Proceedings of the Royal Society A **276**, 238 (1963).

[31]C. Durkan, Contemporary Physics **45**, 1 (2004).

[32]N. Lorente and J.-P. Gauyacq, Phys. Rev. Lett. **103**, 176601 (2009).

[33]D. Serrate, P. F. Y. Yoshida, S.-W. Hla, M. Menzel, K. von Bergmann, S. Heinze, A. Kubetzka, and R. Wiesendanger, Nature Nanotechnology **5** (2010).

[34]J. E. Subotnik and A. Nitzan, J. Chem. Phys. **139**, 034103 (2013).

[35]L. D. Landau and E. M. Lifschitz, *Quantum Mechanics, Non-relativistic theory (Volume 3 of a Course in Theoretical Physics)*, 3rd ed. (Pergamon Press, Oxford, UK, 1977) pp. 55–57.

[36]M. Zhuang and M. Ernzerhof, J. Chem. Phys. **120**, 4921 (2004).

[37]M. Ernzerhof, J. Chem. Phys. **135**, 014104 (2011).

[38]R. Brualdi and H. Schneider, Linear Algebra and its Applications **52–53**, 769 (1983), we use a theorem by Sylvester, *c.f.* p. 772, Eqs. (7) and (8) with $k = n-2$, and with notational changes to suit the present work.

[39]P. W. Fowler, B. T. Pickup, T. Z. Todorova, and W. Myrvold, J. Chem. Phys. **131**, 244110 (2009).

[40]A. Cauchy, Oeuvres Complètes, Second Ser. **IX**, 174 (1833).

[41]S. Fiske, *Polynomials, Roots and Interlacing* (ArXiv:math/0612833v2, 2008).

[42]M. B. Monagan, K. O. Geddes, K. M. Heal, G. Labahn, S. M. Vorkoetter, J. McCarron, and D. P, *Maple 18 Programming Guide* (Maplesoft, Waterloo ON, Canada, 2014).

[43]E. H. Lieb and F. Y. Wu, Physica A **321**, 1 (2003).

[44]R. Pariser and R. G. Parr, J. Chem. Phys. **21**, 466 (1953).

[45]R. Pariser and R. G. Parr, J. Chem. Phys. **21**, 767 (1953).

[46]S. K. Maiti, J. Appl. Phys. **117**, 024306 (2015).

[47]S. K. Maiti, Reviews in Theoretical Science **4**, 179 (2016).

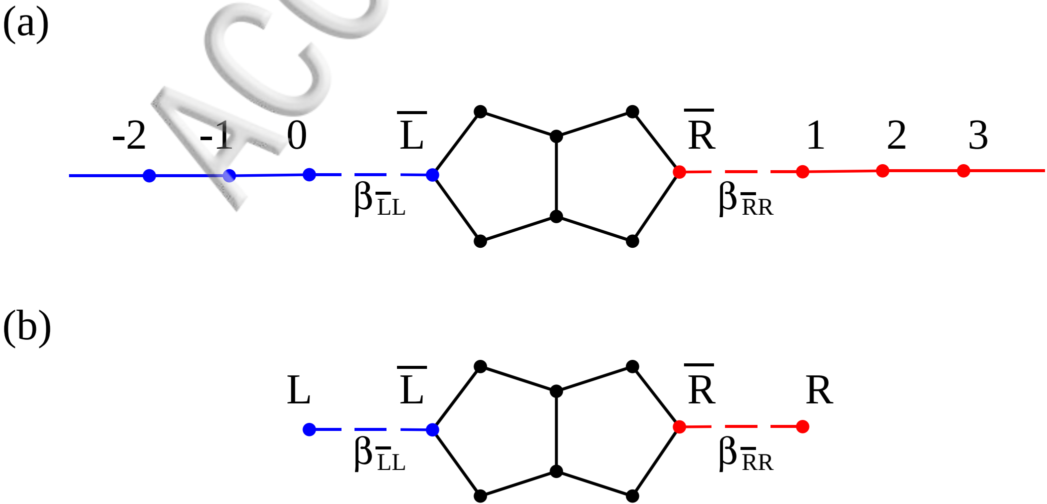
(a)
-2
-1
0
$\bar{L}$
$\bar{R}$
1
2
3
$\beta_{\bar{L}L}$
$\beta_{\bar{R}R}$
(b)
L
$\bar{L}$
$\bar{R}$
R
$\beta_{\bar{L}L}$
$\beta_{\bar{R}R}$

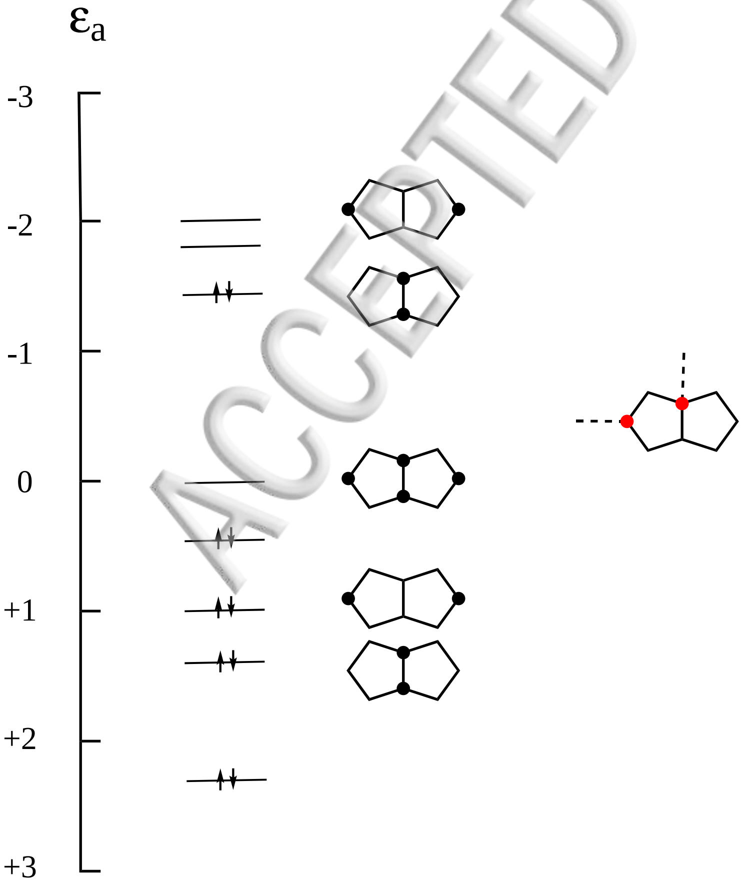
ε_a
-3
-2
-1
0
+1
+2
+3

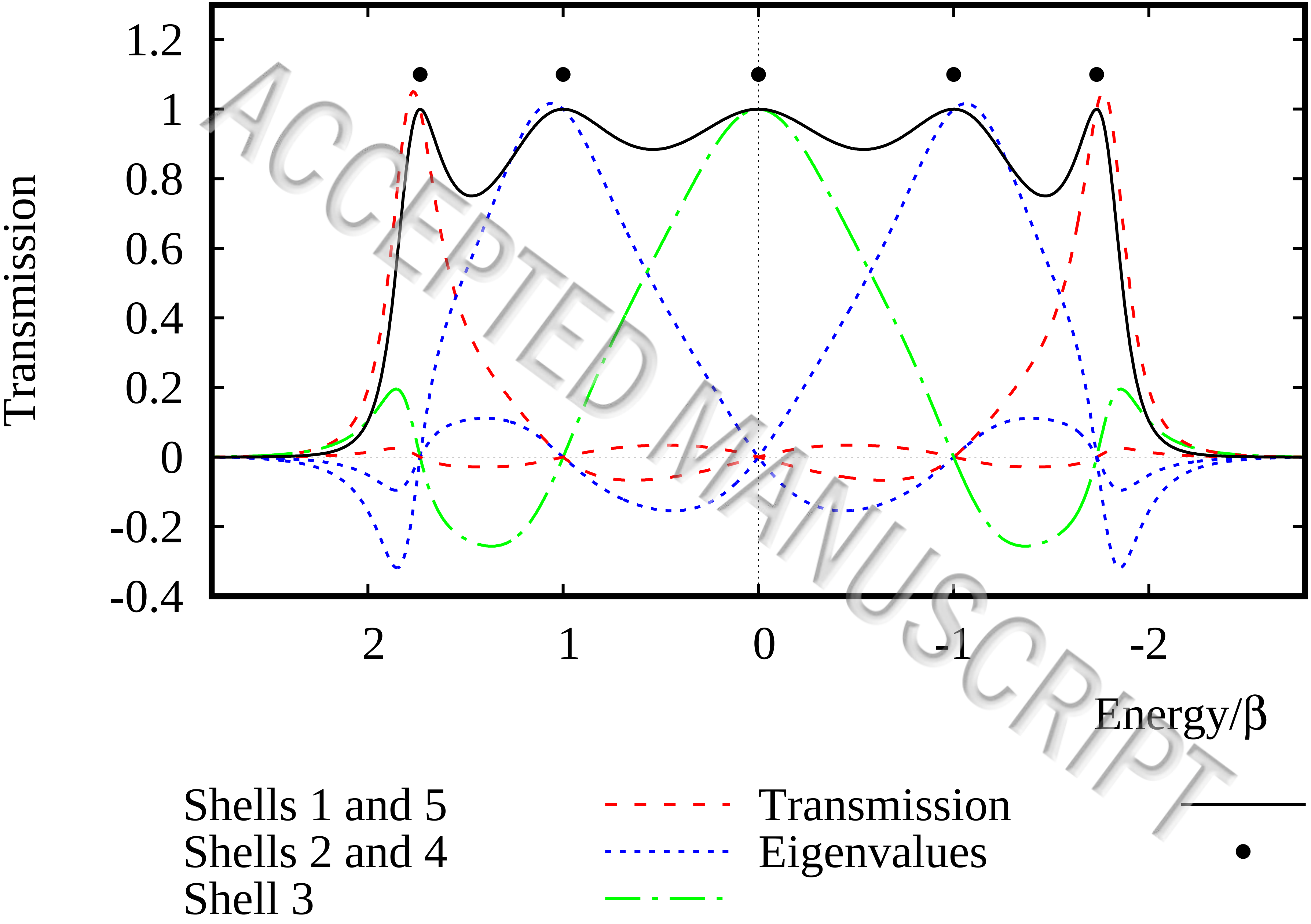
1.2
1
0.8
0.6
0.4
0.2
0
-0.2
-0.4
Transmission
2
1
0
-1
-2
Energy/β
Shells 1 and 5
Shells 2 and 4
Shell 3
Transmission
Eigenvalues ●

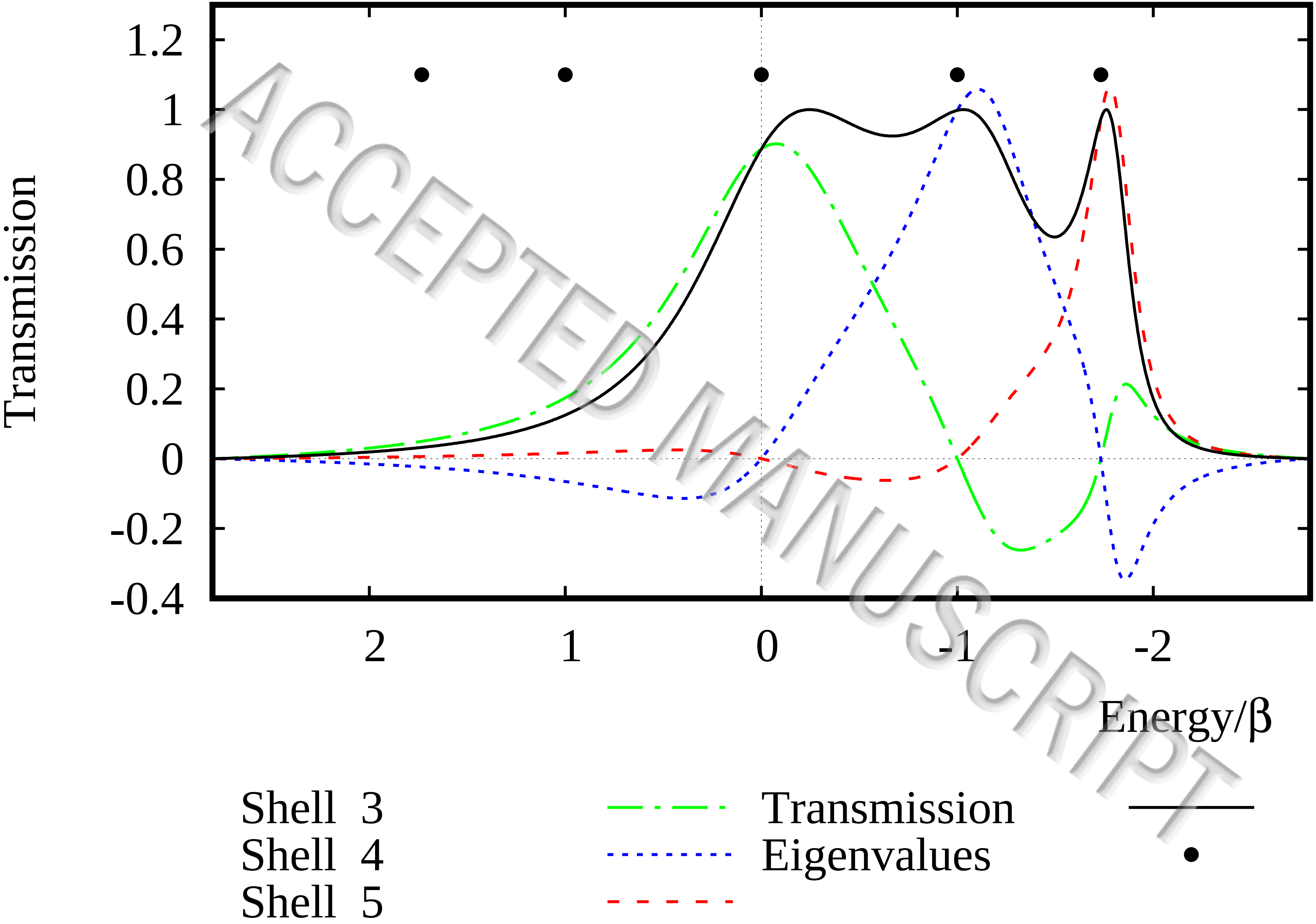
1.2
1
0.8
0.6
0.4
0.2
0
-0.2
-0.4
Transmission
2
1
0
-1
-2
Energy/β
Shell 3
Shell 4
Shell 5
Transmission
Eigenvalues

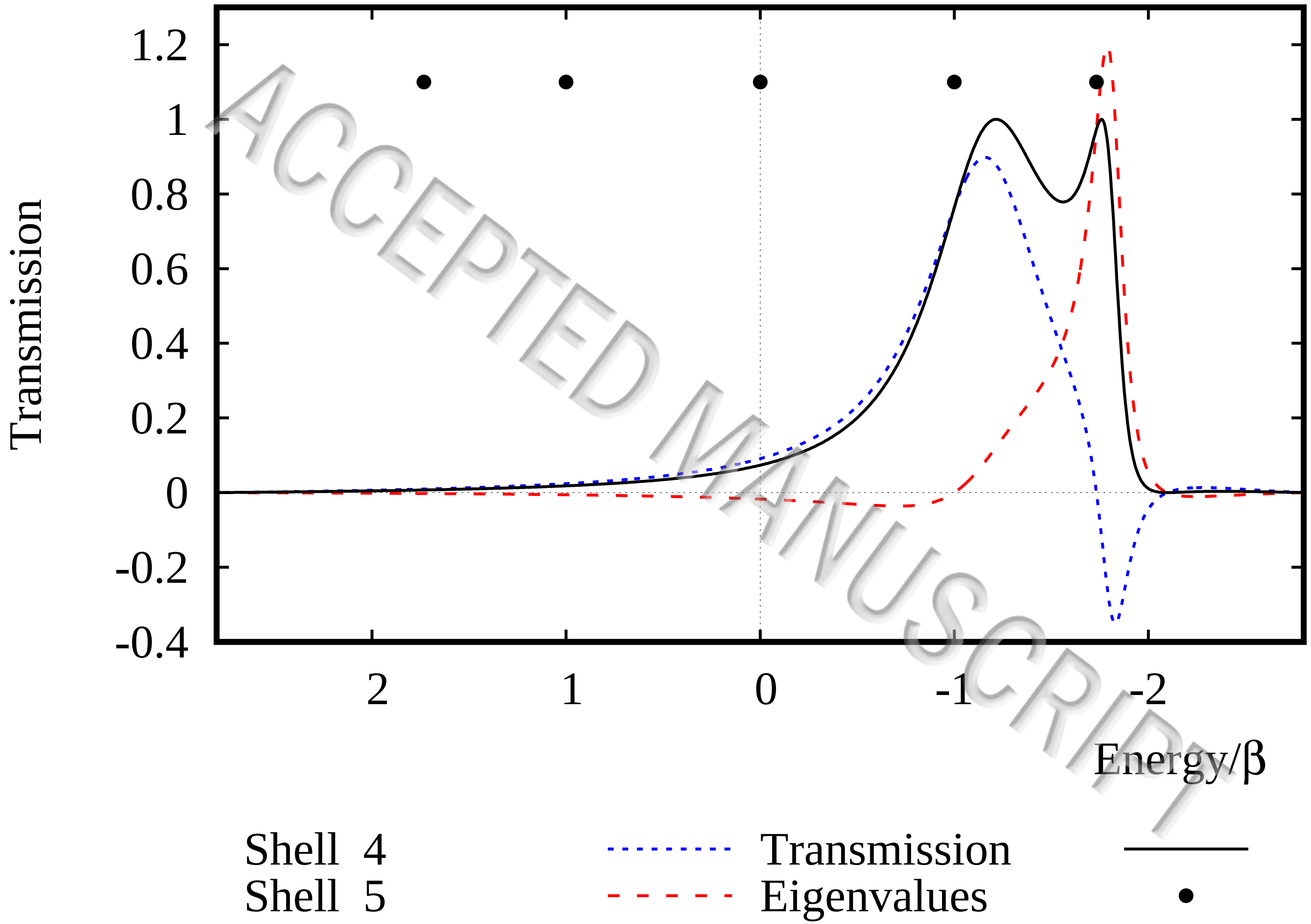
Transmission
1.2
1
0.8
0.6
0.4
0.2
0
-0.2
-0.4
2
1
0
-1
-2
Energy/β
Shell 4
Shell 5
Transmission
Eigenvalues

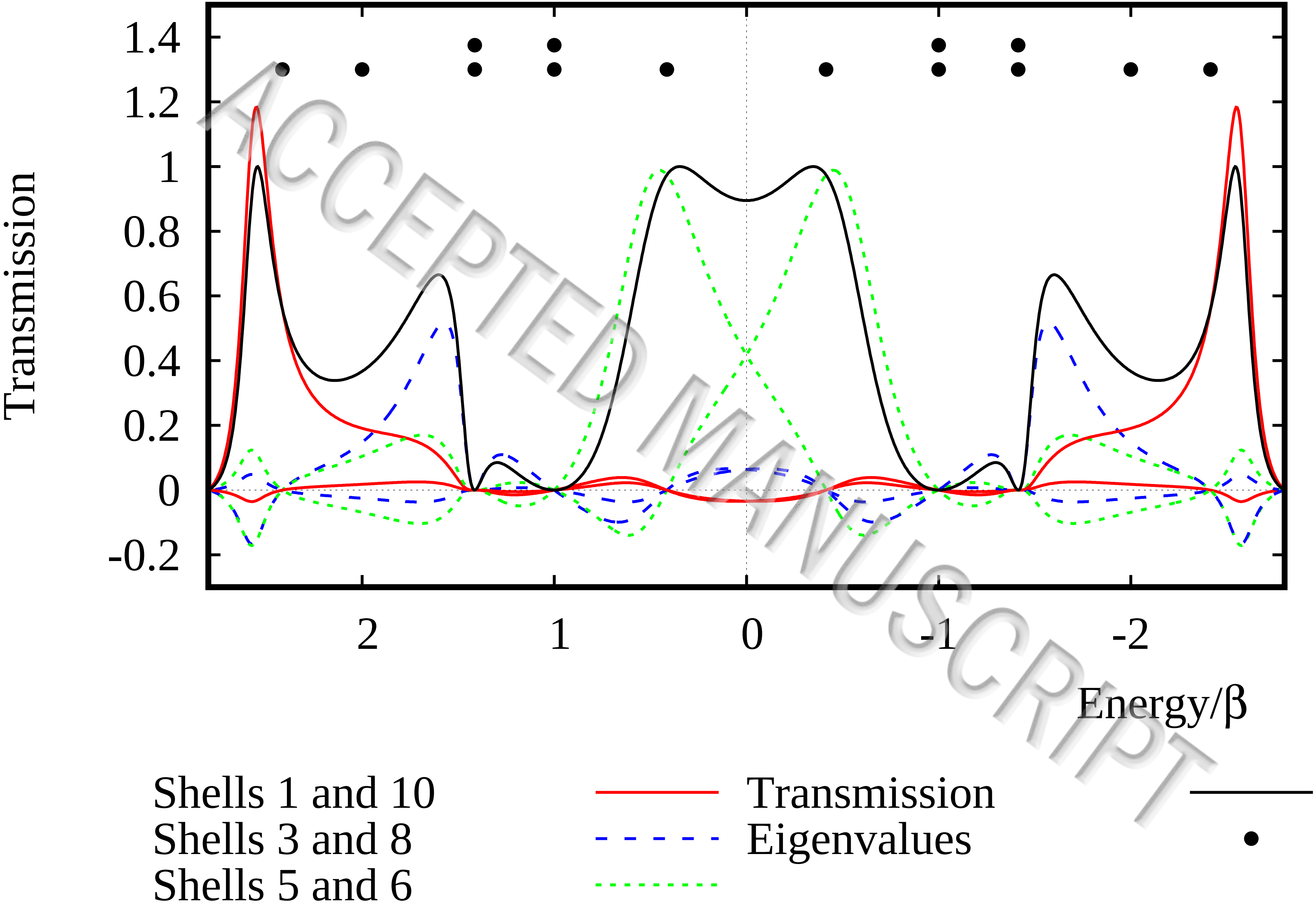
Transmission
1.4
1.2
1
0.8
0.6
0.4
0.2
0
-0.2
2
1
0
-1
-2
Energy/β
Shells 1 and 10
Shells 3 and 8
Shells 5 and 6
Transmission
Eigenvalues ●

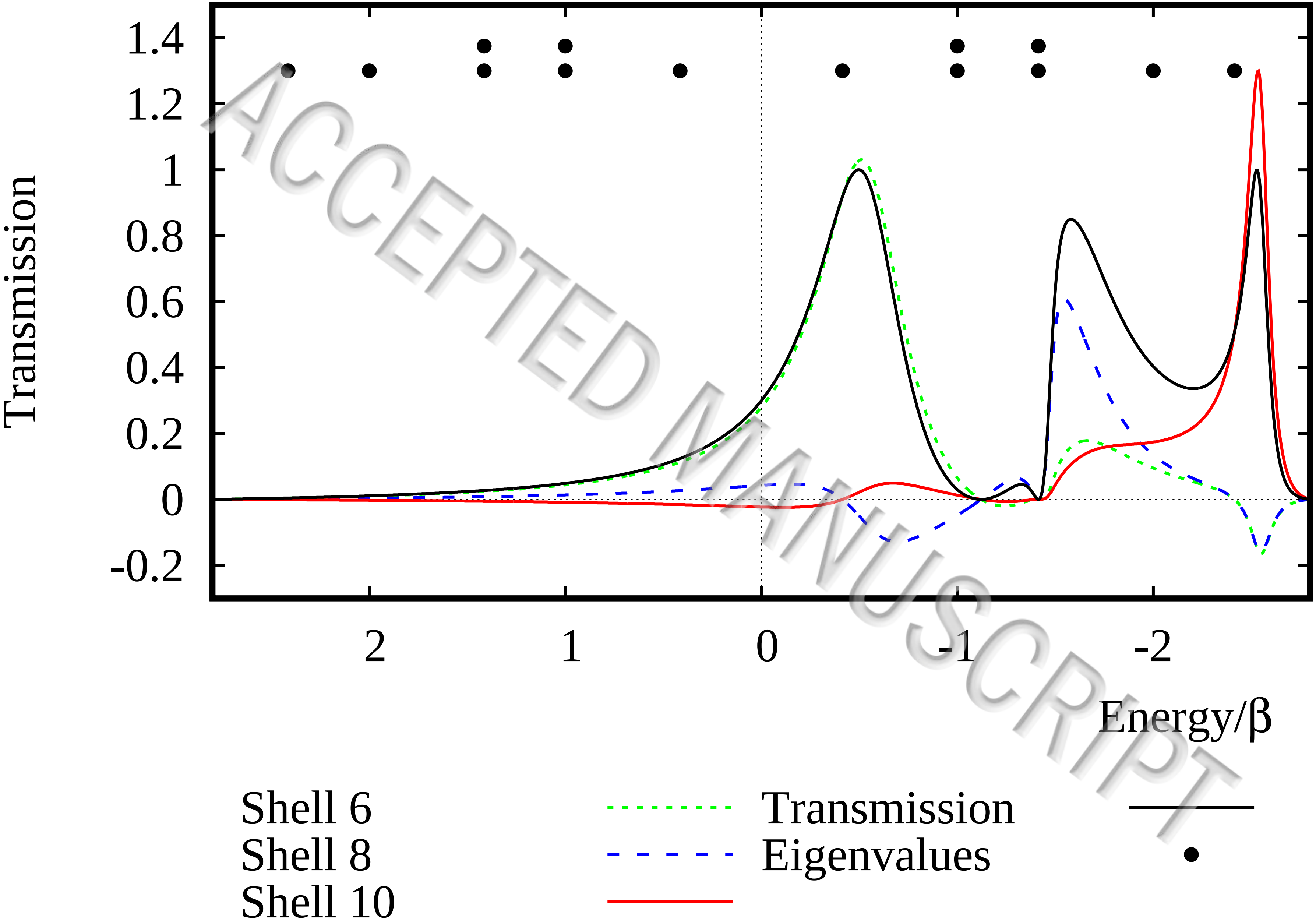
Transmission
1.4
1.2
1
0.8
0.6
0.4
0.2
0
-0.2
2
1
0
-1
-2
Energy/β
Shell 6
Shell 8
Shell 10
Transmission
Eigenvalues

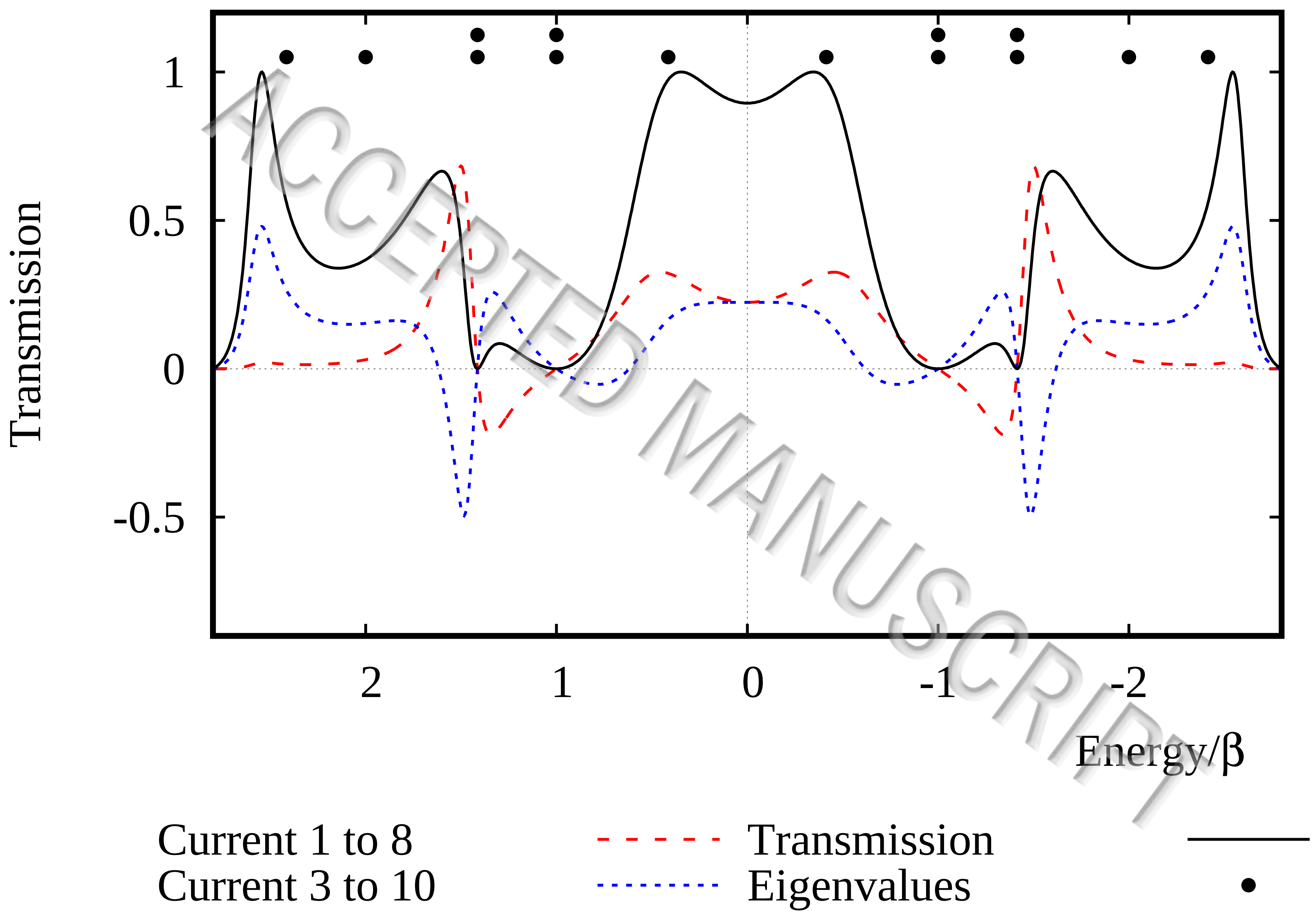
Transmission
1
0.5
0
-0.5
2
1
0
-1
-2
Energy/β
Current 1 to 8
Current 3 to 10
Transmission
Eigenvalues

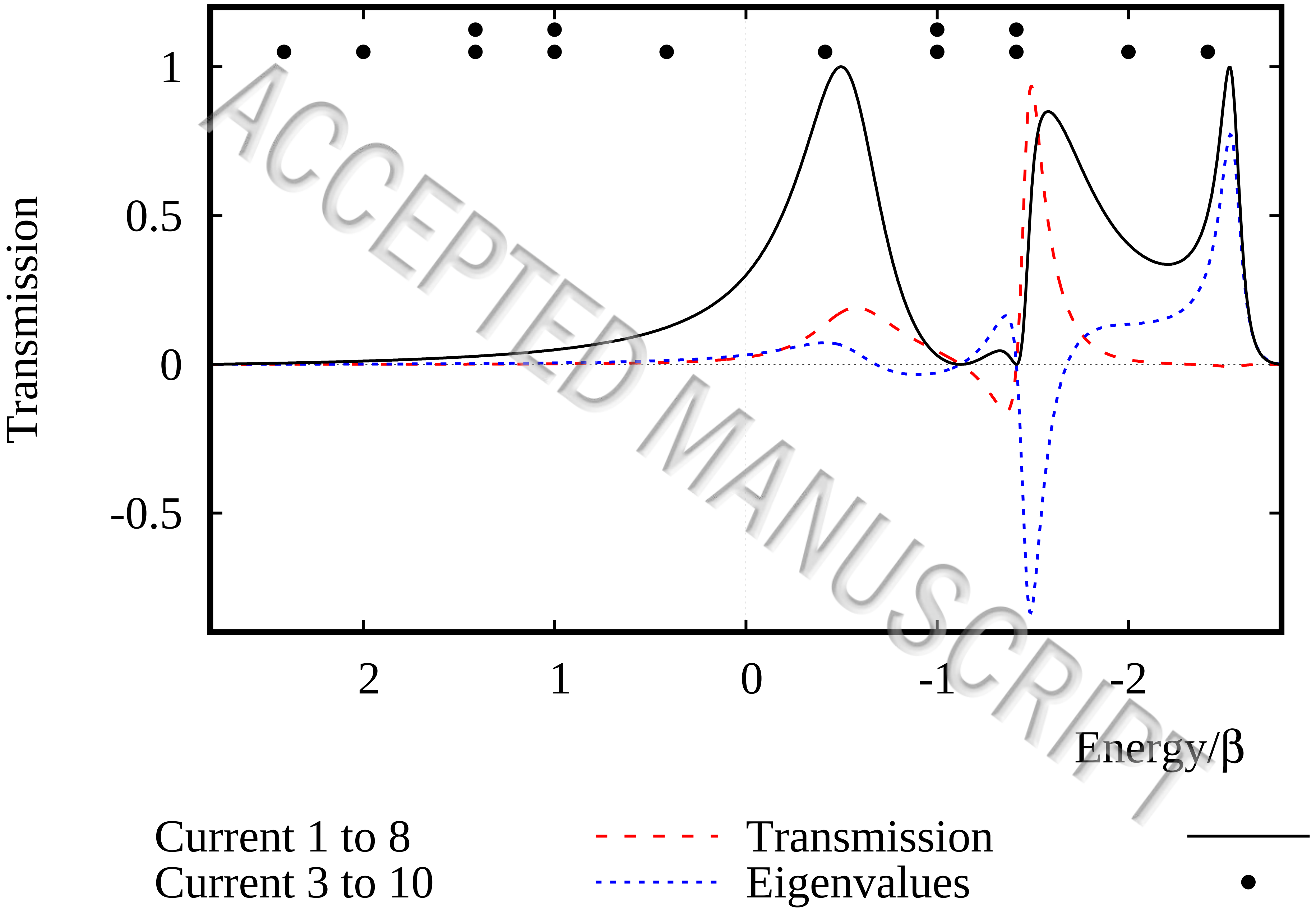
1
0.5
0
-0.5
Transmission
2
1
0
-1
-2
Energy/β
Current 1 to 8
Current 3 to 10
Transmission
Eigenvalues

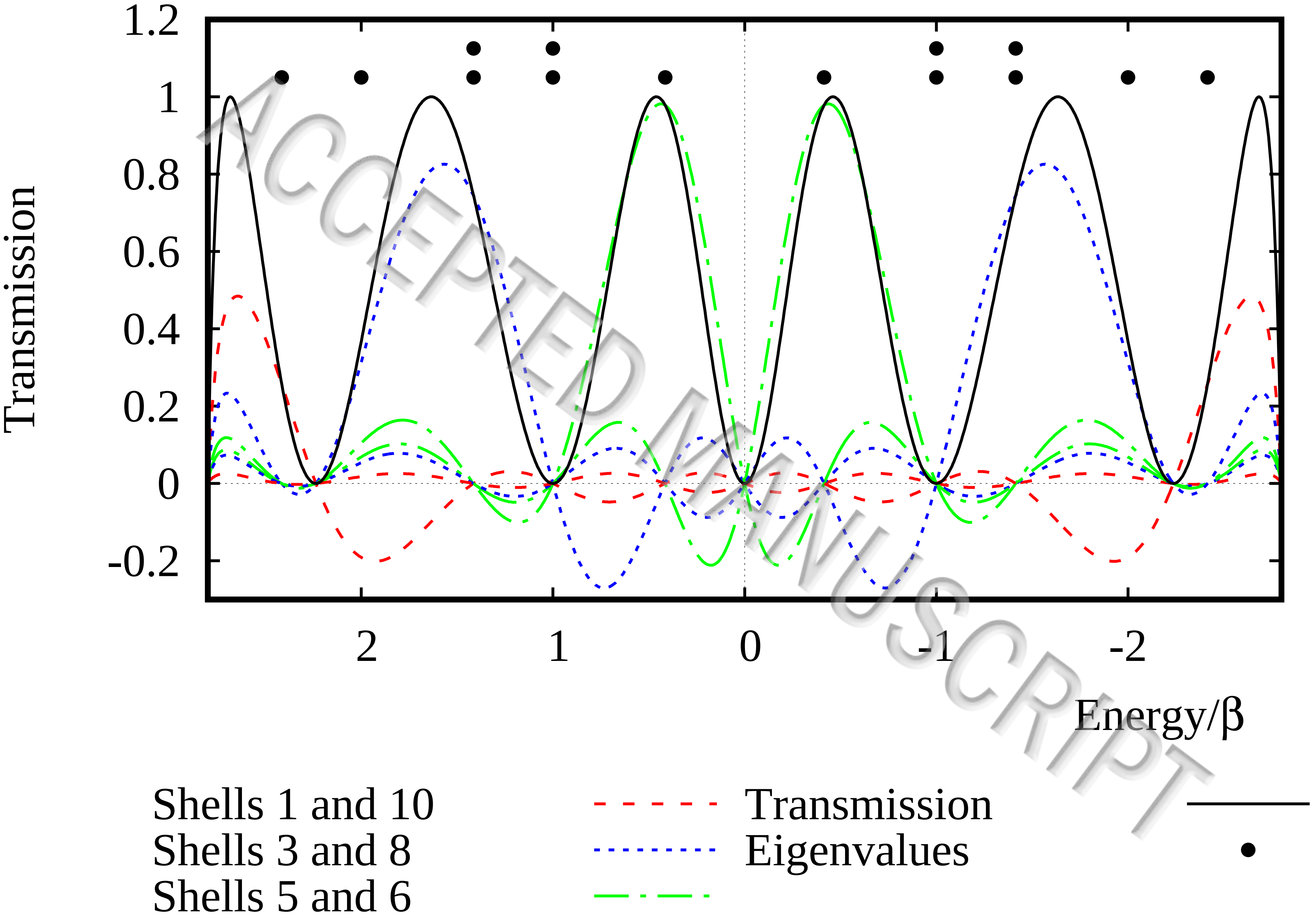
Transmission
1.2
1
0.8
0.6
0.4
0.2
0
-0.2
2
1
0
-1
-2
Energy/β
Shells 1 and 10
Shells 3 and 8
Shells 5 and 6
Transmission
Eigenvalues

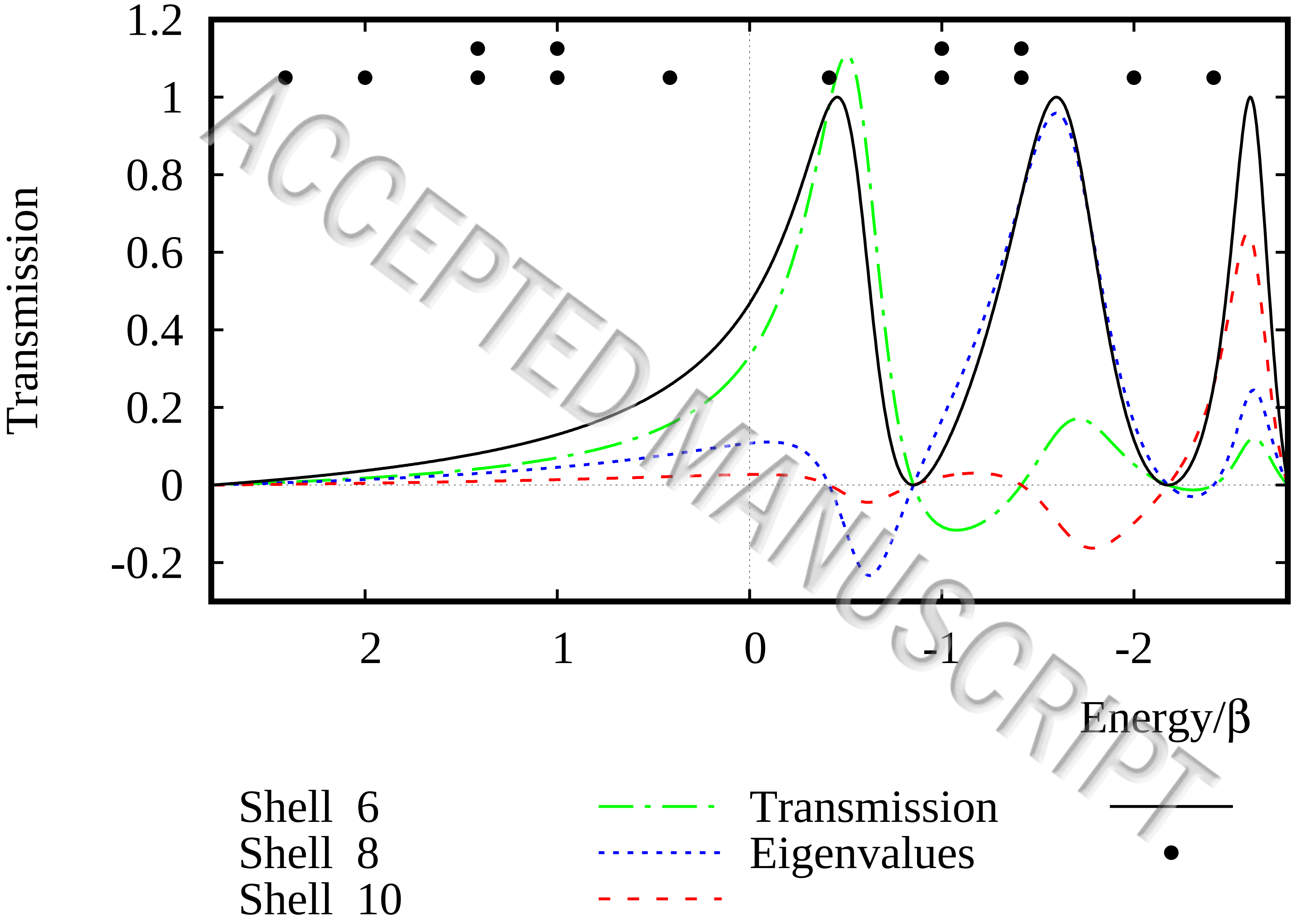
1.2
1
0.8
0.6
0.4
0.2
0
-0.2
Transmission
2
1
0
-1
-2
Energy/β
Shell 6
Shell 8
Shell 10
Transmission
Eigenvalues
●